

UC Berkeley
SEMM Reports Series

Title

Numerical Problems in Nonlinear Analysis of Reinforced Concrete

Permalink

<https://escholarship.org/uc/item/4fm9371w>

Author

Muller, Gunter

Publication Date

1977-09-01

REPORT NO.
UCSESM 77-5

STRUCTURES AND MATERIALS RESEARCH
DEPARTMENT OF CIVIL ENGINEERING

NUMERICAL PROBLEMS IN NONLINEAR ANALYSIS OF REINFORCED CONCRETE

by

GUENTER MUELLER

Report to
National Science Foundation
NSF Grant ENG 77-00146

SEPTEMBER 1977

STRUCTURAL ENGINEERING AND STRUCTURAL MECHANICS
COLLEGE OF ENGINEERING
UNIVERSITY OF CALIFORNIA
BERKELEY, CALIFORNIA 94720

Structures and Materials Research
Department of Civil Engineering
Division of Structural Engineering
and
Structural Mechanics

NUMERICAL PROBLEMS IN NONLINEAR ANALYSIS
OF REINFORCED CONCRETE

by

Guenter Mueller
Visiting Scholar

Faculty Investigator: A. C. Scordelis

Prepared under the Sponsorship of
National Science Foundation
Grant ENG 77-00146

College of Engineering
Office of Research Services
University of California
Berkeley, California

September 1977

TABLE OF CONTENTS

	<u>Page</u>
TABLE OF CONTENTS	i
ACKNOWLEDGEMENTS	ii
NOTATIONS	iii
1. INTRODUCTION	1
2. BRIEF DESCRIPTION OF THE COMPUTER PROGRAM NOTACS	3
3. EXAMPLE 1 - REINFORCED CONCRETE ROD	8
3.1 Incremental Method, Hand Calculation	8
3.2 Combined Incremental/Iterative Method, Hand Calculation	9
3.3 Solution with Program NOTACS	10
3.4 Numerical Experiences	10
3.5 Tension Stiffening Effects	11
4. EXAMPLE 2 - REINFORCED ROD SYSTEM	19
4.1 Hand Calculation	19
4.2 Solutions with Program NOTACS	19
4.2.1 Incremental/Iterative Procedure, Curve No. 2	19
4.2.2 Incremental/Iterative Procedure, Curve No. 3	20
4.2.3 Incremental Procedure, Curve No. 4	20
4.2.4 Incremental/Iterative Procedure, Curve No. 5	20
4.3 Numerical Experiences	20
5. EXAMPLE 3 - REINFORCED CONCRETE BEAM	28
5.1 Nonlinear Analysis	29
6. EXAMPLE 4 - REINFORCED CONCRETE SLAB	38
6.1 Nonlinear Analysis	39
6.2 Hand Calculation (Control)	40
7. RECOMMENDATIONS FOR EXTENSION OF THE PROGRAM AND FOR FURTHER STUDIES	49
8. REFERENCES	52

ACKNOWLEDGEMENTS

The author spent 14 months in Berkeley under the sponsorship of the Deutsche Forschungsgemeinschaft (German Science Foundation).

The author wishes to express his deepest appreciation and gratitude to Professor A. C. Scordelis for his encouragement, friendship and instructive discussions during that time. Gratitude is due also to the staff of the SESM Division for their kind hospitality.

The financial assistance for the computer analyses provided by the National Science Foundation, under Grant No. ENG 77-00146, and by the Deutsche Forschungsgemeinschaft are both highly acknowledged.

Finally, the author is very much obliged to the services of the Computer Centers at the University of California, Berkeley, and the Lawrence Berkeley Laboratory.

NOTATIONS

x,y,z	coordinate system
u,v,w	displacements in x,y,z directions
CST-element	constant <u>s</u> train <u>t</u> riangle (membrane) element with 6 DOF
LCCT9-element	<u>l</u> inearly <u>c</u> onstrained <u>c</u> urvature <u>t</u> riangle (bending-) element with 15 DOF
DOF	degree of freedom

Concrete Properties

E_0	uniaxial initial tangent modulus
f'_c	uniaxial compressive strength
f'_t	uniaxial tensile strength
ϵ_c	strain corresponding to f'_c
ϵ_{cu}	ultimate strain in compression
ϵ_{tu}	ultimate strain in tension
ν	Poisson's ratio
β	cracked shear constant ($0.0 \leq \beta \leq 1.0$)

Steel Properties

E_s	initial tangent modulus
E_{sh}	strain-hardening modulus
f_y	yield stress
σ_c	stress in concrete
σ_s	stress in steel
A_c	area of concrete cross section
A_s	area of steel cross section
$\rho = \frac{A_s}{A_c}$	reinforcement ratio

1. INTRODUCTION

This investigation covers an intensive study of the application of the program NOTACS (Nonlinear Time-dependent Analysis of Concrete Structures) developed by Kabir [1]. This program provides a tool to trace the quasi-static nonlinear response of reinforced concrete shear panels, slabs of arbitrary geometry and free form shell-type structures under sustained load conditions. Cracking and time-dependent environmental phenomena such as creep and shrinkage effects are considered. This program represents one of several which have been developed at the University of California for the nonlinear analysis of reinforced and prestressed concrete. This research is under the direction of Professor A. C. Scordelis.

The first objective of the present study is to check the NOTACS program on various systems and to investigate the influence of various convergence criteria on the results obtained. The finite element method used in NOTACS provides the necessary tool for analytical solutions which can replace much of the empirical testing carried out in the past. As pointed out in [2], "much of the research on reinforced concrete structures has been on isolated structural elements (beams, columns, etc.). More recently it has been recognized that attention needs to be focused on integrated structural systems. Complex structures such as multi-cell box girder bridges, dams and prestressed concrete nuclear containment vessels, whose construction involves large expenditures of governmental and private funds, are examples which must be studied as total structures. Experimental studies on these structural systems are very expensive and the empirical approaches of the past are

gradually being replaced by refined analytical methods."

In this report nonlinear analyses are performed for instantaneous loading only. Examples of nonlinear analyses shall be given and compared with solutions based on other procedures as described in the state-of-the-art reports [2], [4], [5], and [6]. At the end of the report recommendations to improve the computer program and suggestions for further studies are given. In a second report [3], reinforced concrete hyperbolic shells are analyzed for both instantaneous and sustained loadings.

2. BRIEF DESCRIPTION OF THE COMPUTER PROGRAM NOTACS

The method of analysis is based on a finite element tangent stiffness formulation coupled with a time step integration scheme. Within a time step, an incremental load procedure, with an iterative approach to solve the equilibrium equations for each load increment, is adopted to trace the nonlinear behavior. All load changes are considered to occur at the beginning of a time step and the resultant state of stress is assumed to prevail throughout the time step. The creep and shrinkage strains are taken as initial strains and are assumed to occur at the end of each time step. The unbalanced forces at the end of each iteration or load increment are carried forward to the following step until a specified convergence is obtained.

Two types of finite elements are implemented in the program: a flat triangular shell element for reinforced concrete shells and a boundary spring element. The shell element (Fig. 2.1) is a combination of a constant strain triangular (CST) membrane element and a linearly constrained curvature triangular (LCCT9) plate bending element. Thus the element has only five degrees of freedom at each node. The in-plane rotation is not considered as a degree of freedom. By constraining the appropriate degree of freedom, the element may be also used for flat panel-type or slab-type structures.

The boundary element is used to limit nodal displacements or rotations to specified values, to compute support reactions, to provide linear-elastic supports at nodes, and to overcome the problem of the missing sixth degree of freedom at coplanar shell nodes. The element is defined by a single directed axis through a specified nodal point

and has an extensional and/or rotational stiffness. Its element stiffness is added directly to the total structural stiffness matrix and hence has no effect on the size or bandwidth of the stiffness matrix.

The reinforced concrete composite is represented as a layered system (Fig. 2.1) consisting of concrete and "equivalent smeared" steel layers. Variations of properties through the depth of the member are due to different materials or levels of deformation. Kirchhoff's assumption of plane sections remaining plane is adopted to interrelate the displacements at various levels through the section depth and thus reduce each layer to a two-dimensional problem.

The material behavior of concrete is characterized by a nonlinear constitutive relationship for the biaxial state of stress. The biaxial state of stress is accounted for by a family of equivalent uniaxial stress-strain curves (Fig. 2.2) which depend on the biaxial stress ratio as suggested by Darwin and Pecknold (see reference in [1]).

Five material properties of concrete must be prescribed for the construction of these curves: the uniaxial initial tangent modulus E_0 , the uniaxial compressive strength f'_c , Poisson's ratio ν , the tensile strength f'_t , and the ultimate strain in tension ϵ_{tu} . These values can be taken either from uniaxial load tests or code recommendations. The maximum compressive stresses σ_{ic} and corresponding strains ϵ_{ic} in the principal directions $i = 1, 2$ are obtained from the biaxial failure envelope of Kupfer and Gerstle and equations proposed by Darwin, Pecknold and Rajagopal (references in [1]).

A very significant property of concrete is its low tensile strength. Tensile cracking reduces the stiffness of the concrete and is a major contributor to the nonlinear behavior of reinforced concrete structures.

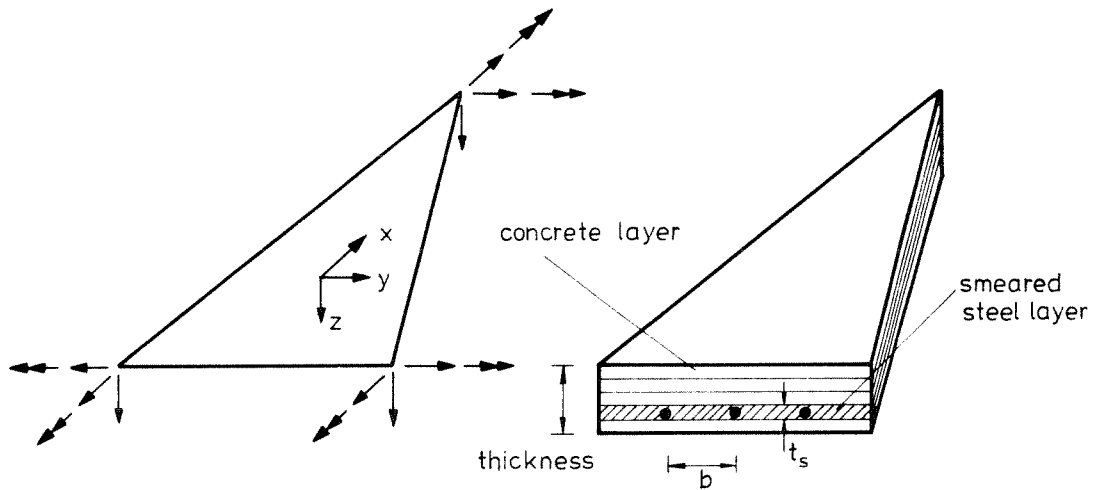


FIG.2.1 COMBINED CST- AND LCCT9- ELEMENT

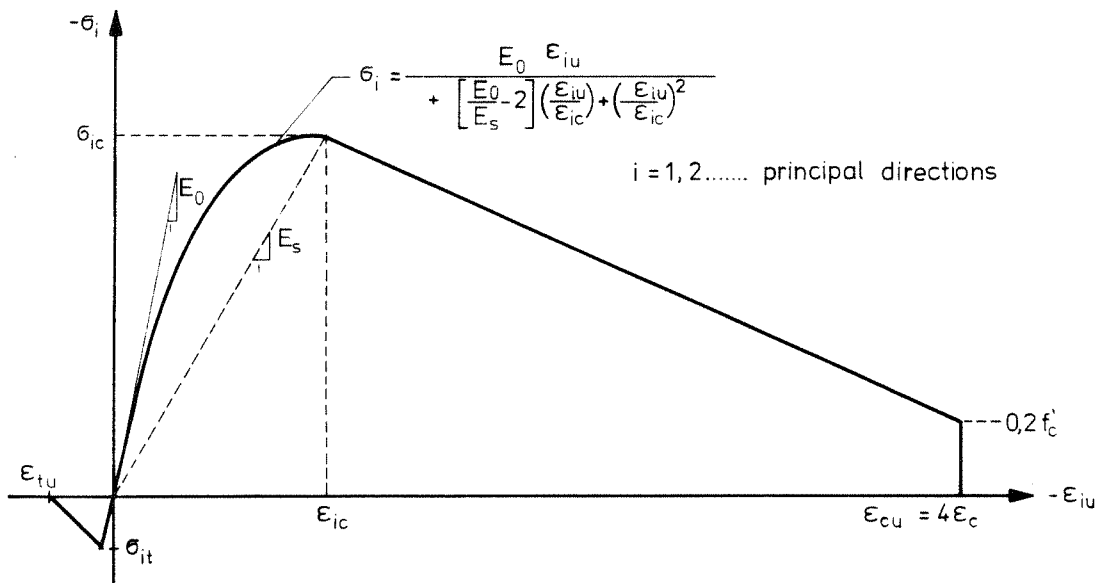


FIG.2.2 EQUIVALENT UNIAXIAL STRESS-STRAIN MODEL FOR CONCRETE

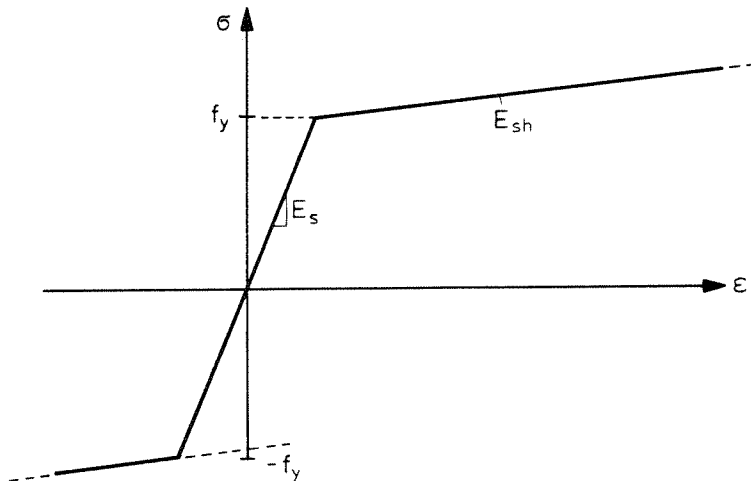


FIG.2.3 STRESS-STRAIN MODEL FOR STEEL

Herein a maximum stress criterion is used to determine concrete failure in tension. Whenever one of the principal stresses exceeds the uniaxial tensile strength of concrete, a crack is assumed to form perpendicular to the direction of that stress and the corresponding tangent modulus is assumed to be zero. Once the concrete is cracked in one direction, the formation of a new crack is restricted to a direction orthogonal to the first crack. To account for the tension stiffening effect of the concrete between cracks, the unbalanced stresses are released gradually depending on the strain level as shown in Fig. 2.2. To estimate the effective shear modulus along the tensile cracks due to the effect of dowel action and aggregate interlock, a cracked shear constant β is introduced. β can be given a value from 0.0 to 1.0. Usually β is chosen to be 0.5.

The steel reinforcement is stressed uniaxially. The material is represented by a bilinear model which may either be elastic-perfectly-plastic or strain-hardening with a Bauschinger type effect as shown in Fig. 2.3.

For concrete, time-dependent effects such as creep and shrinkage are included. The linear superposition method is used to account for the effects of stress history on the creep strain calculations. Variations of creep compliance due to slump of concrete mix, size of members, relative environmental humidity, and high stress or temperature levels are considered on the basis of available experimental data or code recommendations. Creep under biaxial state of stress is represented by the introduction of the creep Poisson's ratio observed in a uniaxial sustained load test. The computational procedure used [1] requires the stress state of only the last time step and is thus very efficient in

the sense that it reduces the computation time and storage considerably. Shrinkage strains are assumed to be uniform in each element. The values of creep and shrinkage at each time step can either be read in from available experimental curves or can be predicted by ACI (American Concrete Institute) recommendations.

3. EXAMPLE 1 - REINFORCED CONCRETE ROD

This example was chosen to check the program NOTACS on a simple problem which also can be solved without computer aid and to acquire some experience in nonlinear analysis. Moreover, the application of some formulas given in the literature accounting for the tension stiffening effect also will be shown.

The structure, its idealization, and the relevant material properties are presented in Fig. 3.1. Material properties are only needed for tension. The system is divided into 6 elements, and the element cross sections consist of one concrete layer and one steel layer.

The problem is first analyzed by hand calculation using an incremental method and a combined incremental iterative method.

3.1 Incremental Method, Hand Calculation

The structure is loaded in increments of 6000 lbs (26.7 kN) (Table 3.1 and Fig. 3.2). At the end of the first increment the concrete is still uncracked; the tensile stresses are less than 471 psi (325 N/cm²). For this reason the initial stiffness in the next increment is the same as before. The stiffness in the third increment is changed because the tensile stresses exceed the concrete tensile strength. Additional loads thereafter can only be carried by the steel reinforcement. The stiffness remains unchanged for the fourth and fifth steps. At the end of the fifth increment, the yield stress is reached. The stiffness is zero in the sixth load increment and displacements become infinite. This method predicted an ultimate load of

$$P_{ult} = 5 (6000) = 30,000 \text{ lbs (133.5 kN)}$$

3.2 Combined Incremental/Iterative Method, Hand Calculation

The first load step is analyzed as before (Fig. 3.2). The equilibrium of the internal and external forces is satisfied. This is not true for the next load step where the concrete is cracking. The portion of the load which until now was carried by the concrete is unbalanced. The unbalanced force (released force) in this step is (Table 3.1):

$$P_{\text{unb}} = 10,452 \text{ lbs (46.5 KN)}$$

In the next load step this unbalanced force must be added to the load increment. This is one way to account for the unbalanced forces. It should be noted that the calculated deflection for the second load step is incorrect even though it is possible to get true values for the additional load increments. Another approach, which is followed here, is to equilibrate the unbalanced internal forces before going to the next load step. This implies an additional deflection of $u_2 = 0.03181 \text{ in. (0.81 mm)}$ in the second load step. With a total deflection of $u_2 = 0.03651 \text{ in. (0.93 mm)}$, the total load of $P_2 = 12,000 \text{ lbs (53.4 KN)}$ can now be transferred by the steel reinforcement. In the third load step, an unbalanced force accrues since the stiffness changes within this load step. The unbalanced force is the difference of the total external load and the yield force:

$$P_{\text{unb}} = (18,000 - 16,320) \text{ lbs} = 1680 \text{ lbs (7.5 KN)}$$

This unbalanced force cannot be equilibrated anymore; therefore, this method predicts an ultimate load of

$$P_{\text{ult}} = 2 (6000) = 12,000 \text{ lbs (53.4 KN)}$$

3.3 Solution with Program NOTACS

The analysis performed in the program corresponds with the combined incremental/iterative method (curve No. 2 in Fig. 3.2). Some intermediate results which show the procedure are given in Fig. 3.3. This figure demonstrates clearly that the set of unbalanced forces can be looked at as self-equilibrating forces which intermediately help to transmit the load. In the iterative procedure within a load increment, these forces have to be put on the structure with negative signs.

3.4 Numerical Experiences

(1) Reinforced concrete is a material with a discontinuous stress-strain relationship. For such a material an equilibrium iteration is of particular importance since even with infinitely small load increments it is not possible to approach the true solution (curve No. 3 in Fig. 3.2). This is not the case for continuous nonlinear stress-strain relations.

(2) The exact value of the ultimate load cannot be determined. The true value is greater than the value of the (n-1)th load step and smaller than the value of the nth step, where n is the load step in which failure occurs. The smaller the increment, the better the approach.

(3) Small increments should also be taken in regions of strong stiffness alterations; otherwise it is not possible to trace the behavior (in the transition zone) accurately.

(4) Problems may arise if the crack load P_{cr} is greater than the yield load P_y (Fig. 3.4) or in other terms if

$$f'_t/f_y > \rho$$

In this case the method may predict the crack load P_{cr} as the ultimate

load and not the lower value P_y . This would occur in this example. For more general problems, the situation is not as bad because some elements, due to bending stresses, will crack in an earlier stage (i.e., the theoretical crack load P_{cr} will not be reached). Nevertheless, for under-reinforced structures this should be kept in mind and the results for the ultimate load should be examined critically.

3.5 Tension Stiffening Effect

The following example shows the effect of several tension stiffening assumptions on the overall behavior of a particular reinforced concrete structure. It is believed that a more comprehensive literature study will provide more information to define the important tension stiffening relation.

In Fig. 3.5 the example taken from [7] is presented. The wall panel has a thickness of 3.93 in. (0.10 m) and is reinforced in two orthogonal directions. The reinforcement ratio in both directions is $\rho = 1\%$. The system is stressed only in tension, hence the following data are sufficient:

For concrete:	$E_o = 3800 \text{ ksi (26,000 N/mm}^2\text{)}$
	$f'_t = 380 \text{ psi (2.6 N/mm}^2\text{)}$
For steel:	$E_s = 30,400 \text{ ksi (210,000 N/mm}^2\text{)}$
	$E_{sh} = 0.0$
	$f_y = 61,000 \text{ psi (420 N/mm}^2\text{)}$

Fig. 3.5(c) presents some proposed relations to account for the contribution of concrete after cracking. Based on these curves the corresponding stress-strain relations of concrete (i.e., the tension stiffening curves) are calculated, Fig. 3.5(d). Curve No. 1 represents

the solution if no contribution of the concrete is taken into account. Curve No. 2 is proposed in [7]. Curve No. 3 is an arbitrary (linear) assumption which, for this particular case, matches the experimental results remarkably well. Curve No. 4 is calculated from the following formula proposed by Rostásy [6]:

$$\epsilon_{s,m} = \epsilon_{s,II} - 0.50 \frac{\sigma_{s,II}^{cr}}{\sigma_{s,II}} \frac{f'_t}{E_s \rho}$$

where

- $\epsilon_{s,m}$ reduced strain of steel due to the contribution of concrete
- $\epsilon_{s,II}$ strain of steel in case of no contribution of concrete
- $\sigma_{s,II}$ stress in steel in case of no contribution of concrete
- $\sigma_{s,II}^{cr}$ as before, at the beginning of cracking

In this way other formulas given in the literature [6,8,9,10] could be used.

TABLE 3.1 EXAMPLE 1 - INCREMENTAL METHOD

INCREMENT	DIMENSIONS	1	2	3	4	5
TOTAL LOAD	lbs	6000	12000	18000	24000	30000
AREA OF CROSS SECTION A_I, A_{II}	sq.in.	18,37	18,37	0,272	0,272	0,272
STIFFNESS K_I, K_{II}	lbs/in.	2548838	2548838	328666	328666	328666
LOAD PICKED UP BY CONCRETE P_c	lbs	5226	10452	0	0	0
LOAD PICKED UP BY STEEL P_s	lbs	774	1548	7548	13548	19548
STRESS IN CONCRETE DUE TO INCR. LOAD ΔP_b	psi	327	327	0	0	0
STRESS IN CONCRETE DUE TO TOTAL LOAD P_b	psi	327	654	0	0	0
STRESS IN STEEL DUE TO INCR. LOAD ΔP_s	psi	2845	2845	22059	22059	22059
STRESS IN STEEL DUE TO TOTAL LOAD P_s	psi	2845	5690	27749	49808	71867
STRAIN DUE TO INCREMENT LOAD ΔP	1	0,000098	0,000098	0,000761	0,000761	0,000761
STRAIN DUE TO TOTAL LOAD P	1	0,000098	0,000196	0,000957	0,001718	0,002479
DEFLECTION DUE TO INCREMENT LOAD ΔP	in.	0,00235	0,00235	0,01826	0,01826	0,01826
DEFLECTION DUE TO TOTAL LOAD P	in.	0,00235	0,00470	0,02296	0,04122	0,05948

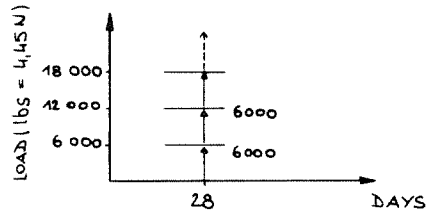
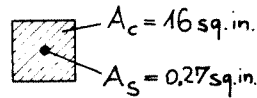
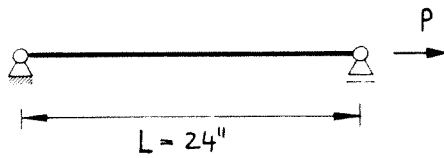
LOAD INCREMENT : $\Delta P = 6000$ lbs

AREA OF CROSS SECTION, UNCRACKED : $A_I = A_c + \frac{E_s}{E_o} \cdot A_s$

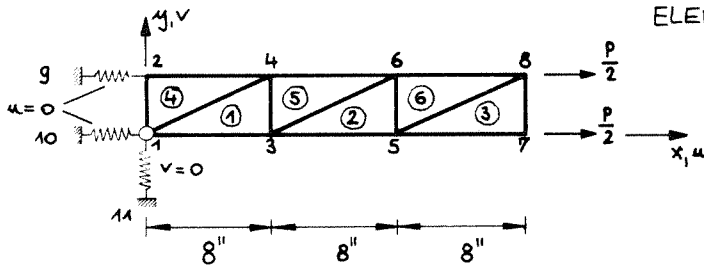
AREA OF CROSS SECTION, CRACKED : $A_{II} = A_s$

STIFFNESS, UNCRACKED : $K_I = A_I \cdot E_o / L$

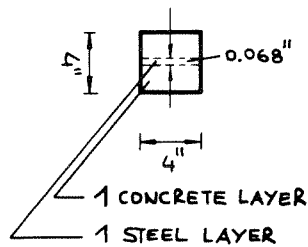
STIFFNESS, CRACKED : $K_{II} = A_{II} \cdot E_s / L$



(a) STRUCTURE AND LOADING

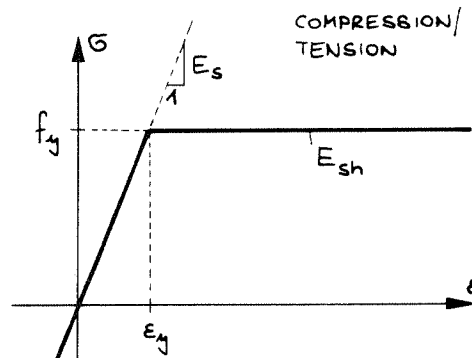
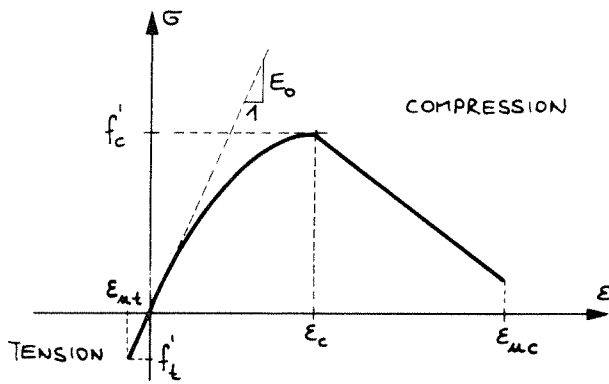


ELEMENT CROSS SECTION



- 0... ELEMENT NUMBERS
- 6 CST-ELEMENTS , 3 BOUNDARY ELEMENTS
- 11 NODES
- 16 DOF

(b) FINITE ELEMENT MESH LAYOUT



$E_0 = 3\,330\,000 \text{ psi} (= 2298 \text{ kN/cm}^2)$
 $f'_t = 471 \text{ psi} (= 325 \text{ N/cm}^2)$
 $\epsilon_{xt} = f'_t / E_0 = 0.14 \text{ ‰}$

$E_s = 29\,000\,000 \text{ psi} (= 20\,010 \text{ kN/cm}^2)$
 $E_{sh} = 0$
 $f_y = 60\,000 \text{ psi} (= 41.4 \text{ kN/cm}^2)$
 $\epsilon_y = f_y / E = 2.07 \text{ ‰}$

(c) MATERIAL PROPERTIES (TENSION ONLY)

FIG. 3.1 EXAMPLE 1 - STRUCTURE, IDEALISATION AND MATERIAL PROPERTIES
 (1" ≡ 1 in. = 25.4 mm)

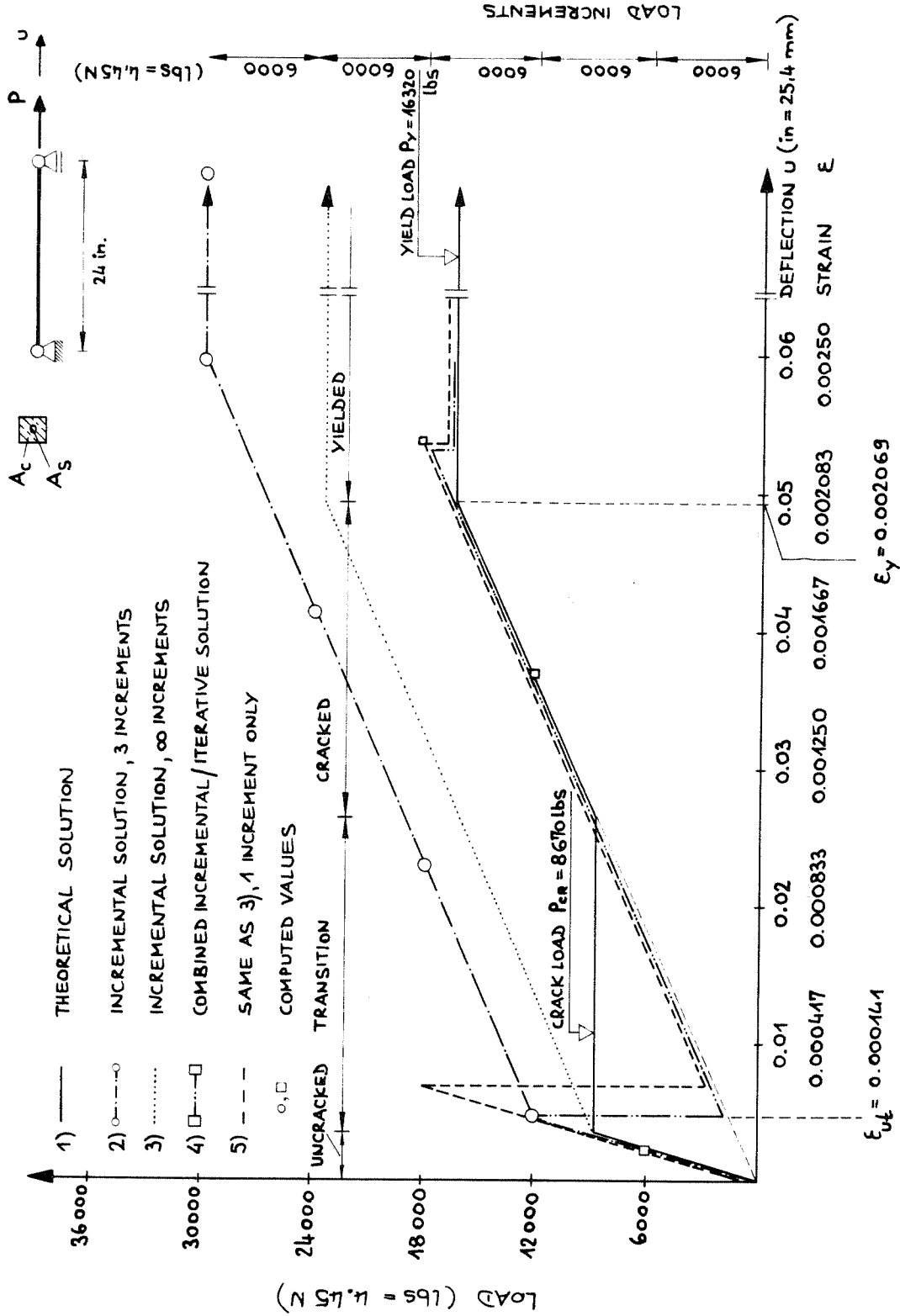


FIG. 3.2 EXAMPLE 1 - LOAD DEFLECTION CURVES

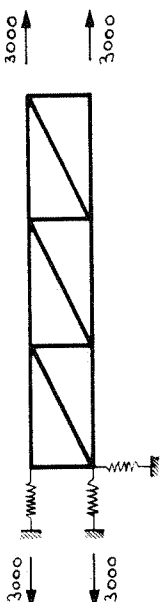
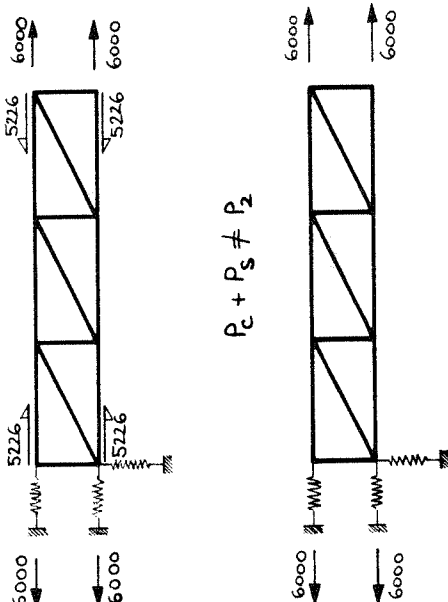
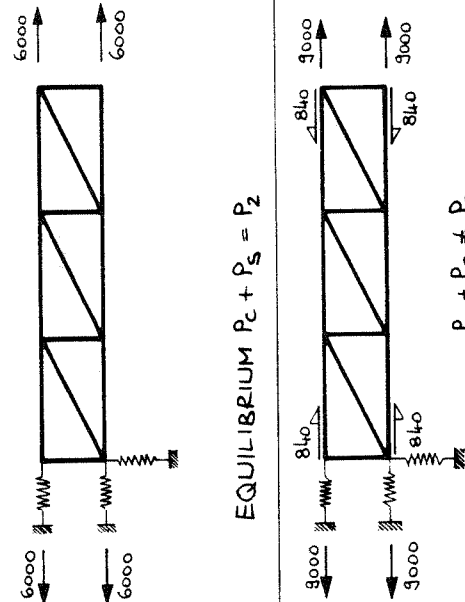
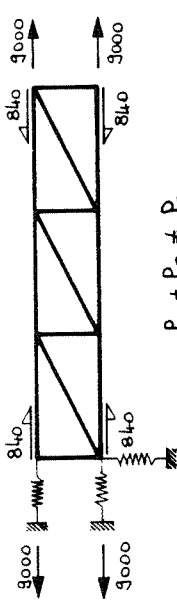
INCREMENT NUMBER	TOTAL LOAD (lbs = 4.45N)	EXTERNAL FORCES UNBALANCED FORCES	σ_c (psi = 0.69 N/cm ²)	σ_s (psi = 0.69 N/cm ²)	P_c (lbs = 4.45N)	P_s (lbs = 4.45N)	ϵ (1)	u (in = 2.54 cm)
1	$P_1 = 6000$	 <p>EXTERNAL FORCES UNBALANCED FORCES</p>	327	2845	5226	774	0.000098	0.00235
2	$P_2 = 12000$	 <p>EQUILIBRIUM $P_c + P_s = P_1$</p> <p>$P_c + P_s \neq P_2$</p>	0	5689	0	1548	0.000196	0.00470
1. ITERATION		 <p>EQUILIBRIUM $P_c + P_s = P_2$</p> <p>$P_c + P_s \neq P_3$</p>	0	44120	0	12000	0.0004521	0.03651
3	$P_3 = 18000$	 <p>EQUILIBRIUM $P_c + P_s = P_2$</p> <p>$P_c + P_s \neq P_3$</p>	0	6000 = YIELD STRESS	0	16320	0.002282	0.05477

FIG 3.3 EXAMPLE 1 - SOLUTION PROCEDURE, PROGRAM NOTACS

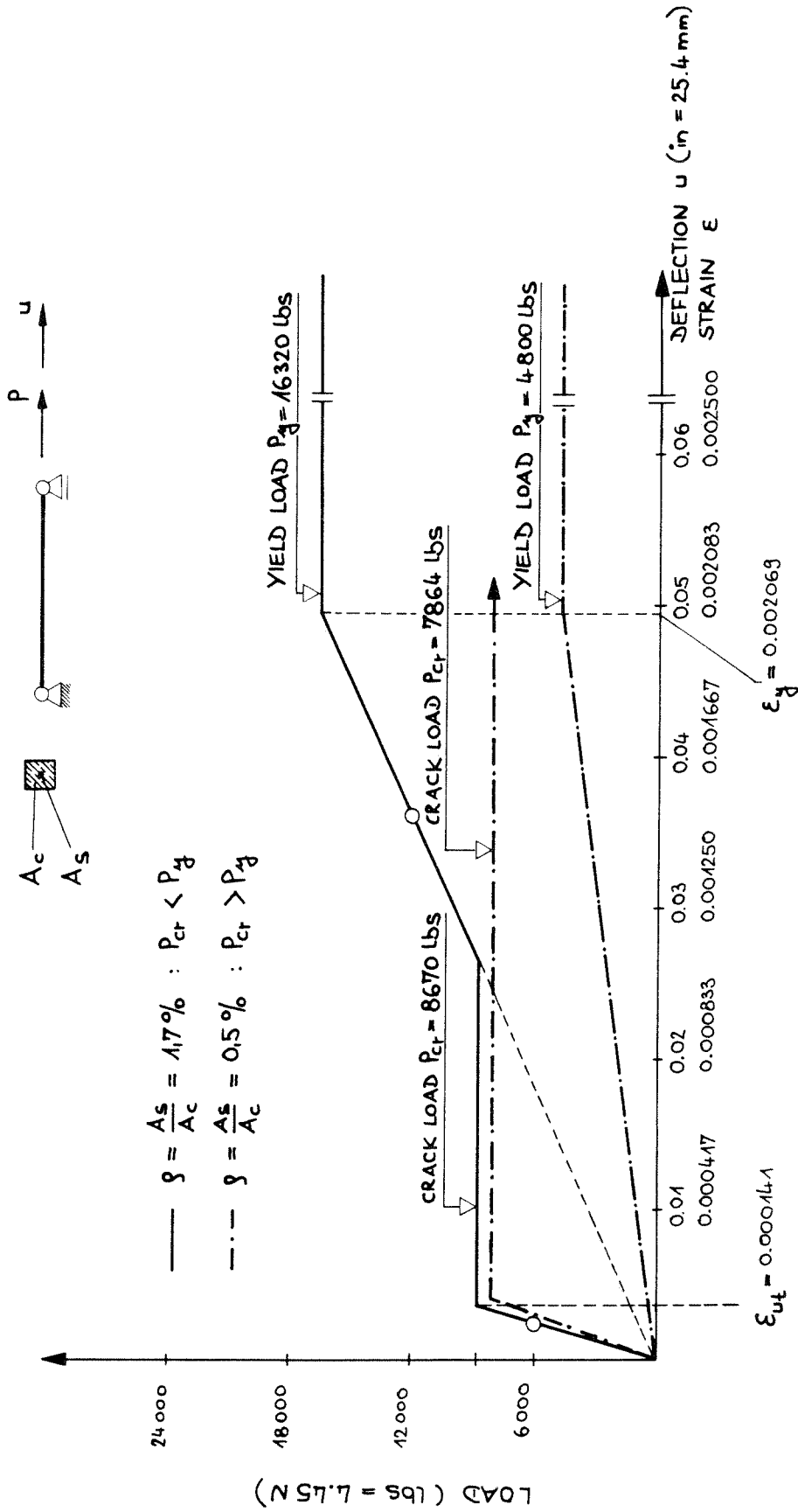
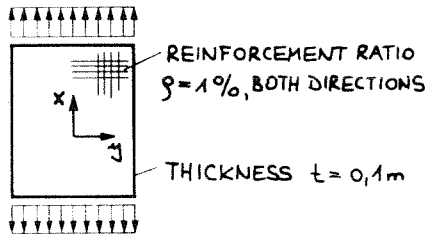
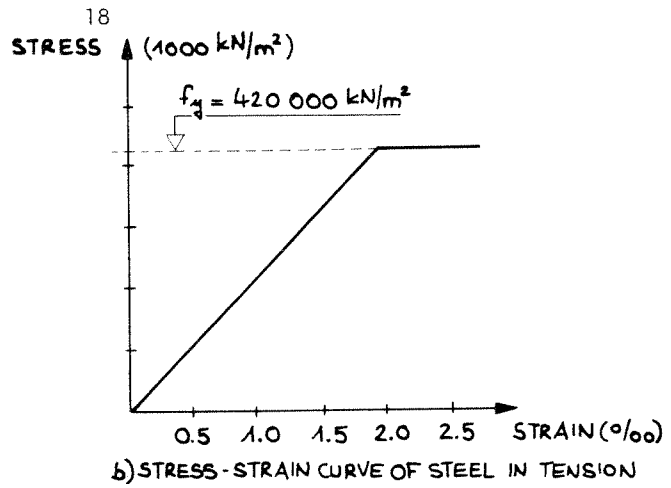


FIG 3.4 EXAMPLE 1 - LOAD-DEFLECTION CURVE FOR DIFFERENT REINFORCEMENT RATIOS



a) STRUCTURE AND LOADING

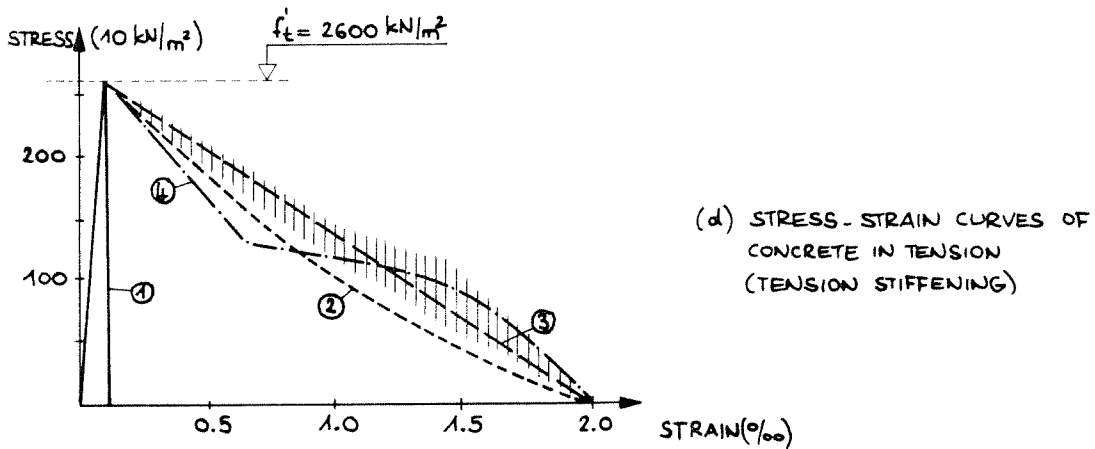
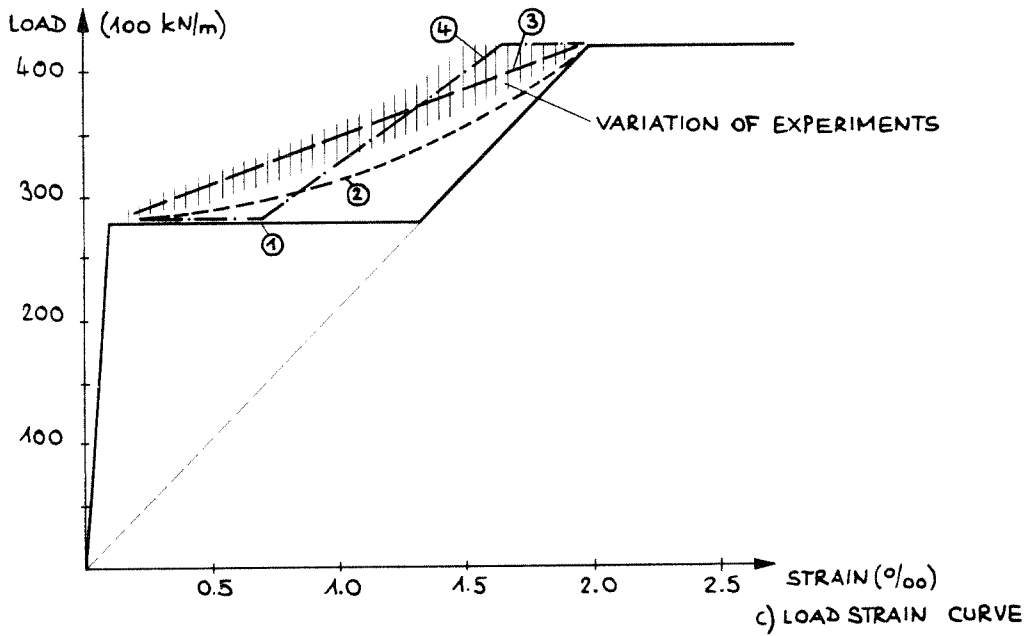


FIG 3.5 TENSION STIFFENING EFFECT

4. EXAMPLE 2 - REINFORCED ROD SYSTEM

This example was chosen for the same reason as the first one; therefore, a hand calculation which allows the control of the program is still feasible. The structure (Fig. 4.1) consists of three reinforced concrete rods with stiffness ratios of 1 : 1/2 : 1/3.

4.1 Hand Calculation

First the load-deflection (strain) curves of the single bars are constructed (Fig. 4.2) using the information noted in Table 4.1. They are characterized mainly by the crack load and the yield load. Crack load, yield load, and corresponding strains are the same as for Example 1. The same holds for the deflections of bar 1. The values for bars 2 and 3 follow from the stiffness ratios. The load deflection curve of the total system results from superposition of the single-load deflection curves. The superposition is performed in Table 4.2 and graphically displayed in Fig. 4.2. The ultimate load is reached when the deflection exceeds 0.04966 in. (1.26 mm), hence the ultimate load is

$$P_{ult} = 3 (16,320) = 48,960 \text{ lbs (218 KN)}$$

4.2 Solutions with Program NOTACS (Fig. 4.3)

4.2.1 Incremental/Iterative Procedure, Curve No. 2

The load increment is chosen as $P = 12,500 \text{ lbs (55.6 KN)}$. In the first step, the system remains uncracked. Within the second step, all bars turn to the cracked state (i.e., all elements change their stiffness within this increment). Theoretically, three iterations are necessary, but numerically, depending on the tolerances, more iterations

may be required. In the third step, two iterations are required; and, finally, in the fourth step the system fails.

Since an insight into the action of the unbalanced forces is important, they are once more represented in Fig. 4.4. There it is clearly demonstrated that only in the "pathological" areas self-equilibrating forces are superimposed to "help" the structure carry the load.

4.2.2 Incremental/Iterative Procedure, Curve No. 3

The procedure is the same as in Section 4.2.1 except only one iteration within each increment is allowed. The result shows quite a discrepancy from the true solution and emphasizes the importance of the equilibrium at the end of each load step.

4.2.3 Incremental Procedure, Curve No. 4

Even more dramatically this solution shows the importance of the equilibrium iteration. A pure incremental method leads to poor and even unrealistic results. At least the unbalanced forces should be transferred to the next load step.

4.2.4 Incremental/Iterative Procedure, Curve No. 5

Curve No. 5 is a solution including a tension stiffening effect. It is assumed that the concrete contributes up to an ultimate strain in tension of $\epsilon_{tu} = 0.0005$. It follows that a much greater number of iterations are required in the second load step.

4.3 Numerical Experiences

(1) Care must be taken so that during any one load increment not too many elements change their stiffness (e.g. by cracking) otherwise the required iterations for convergence may last too long.

(2) Unbalanced forces do not necessarily become smaller by increasing the number of iterations. Oscillations may occur due to the discontinuous material law in tension. An equilibrium state may be nearly reached, however, if in the next iteration new unbalanced forces are released which have to be transferred to support areas, a new iteration cycle to attain equilibrium may be initiated.

(3) Unbalanced forces, at the end of the iterations in one load increment, must be carried over to the next load increment. Residual unbalanced forces always exist since the state of equilibrium is not a true one but is one defined by specified tolerances or number of iterations.

(4) It can be observed that unbalanced forces are created not only in the direction of the load but also perpendicular to it.

(5) The computer program provides two options for the convergence criteria with respect to the iterations: a displacement convergence criterion and a force convergence criterion. For both criteria, absolute values or percentages of already obtained solutions can be set as convergence limits. The computation of several examples, all of which are not included in this report, has shown that it is not reasonable to control all values but only the more significant ones. In the case of the rod system, only the extensional deflections should be controlled, otherwise according to the differences of great numbers, the iteration cycle will be unnecessarily prolonged or stopped too early. From an engineering point of view, the force convergence criterion is preferable to the deflection criterion, because equilibrium is more nearly satisfied. But on the other hand, for general structures it is difficult to estimate the influence of errors in unbalanced nodal forces. Therefore, it is

recommended that the displacement convergence criterion be specified and a print out of the unbalanced forces be given to compare them with the total applied nodal forces.

(6) It is recommended that a linear analysis be performed prior to the nonlinear analysis. This is especially important for larger problems. With a linear analysis, the load level where cracking might start can be estimated and, thus, provides insight regarding where smaller load increments should be used.

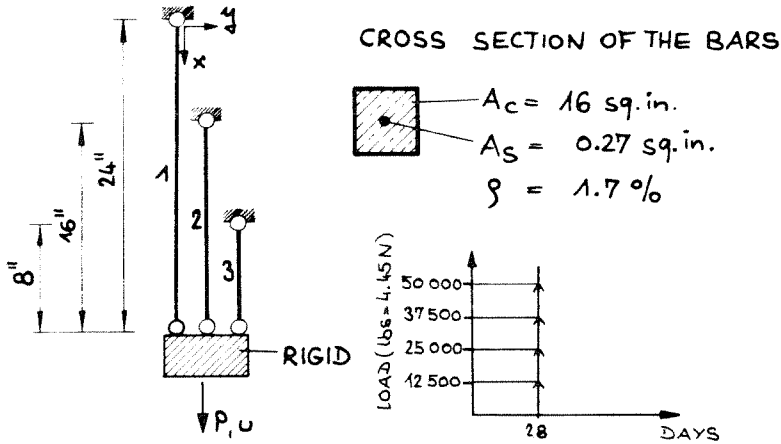
TABLE 4.1 EXAMPLE 2 - CHARACTERISTIC VALUES OF SINGLE BARS

BAR NUMBER	1	2	3
CRACK LOAD (lbs = 4.45N)	8670	8670	8670
CORRESPONDING STRAIN (ϵ)	0.000141	0.000141	0.000141
CORRESPONDING DEFLECTION (in = 25,4 mm)	0.00339	0.00226	0.00113
YIELD LOAD (lbs = 4.45N)	16320	16320	16320
CORRESPONDING STRAIN (ϵ)	0.002069	0.002069	0.002069
CORRESPONDING DEFLECTION (in = 25,4 mm)	0.04965	0.03310	0.01655

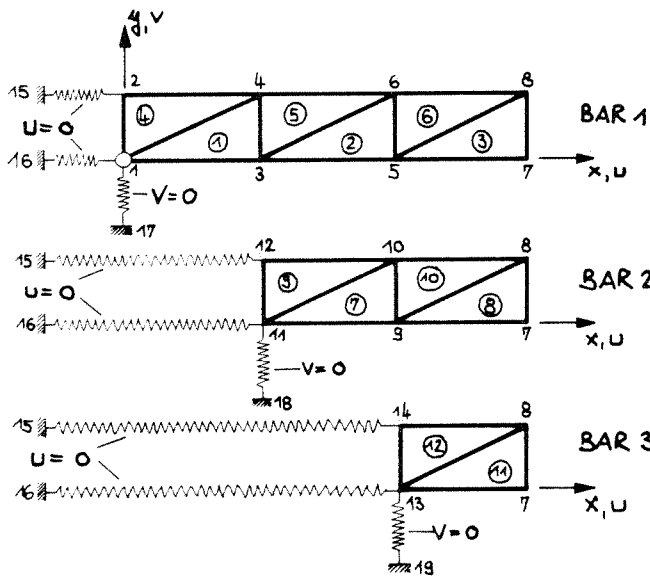
TABLE 4.2 EXAMPLE 2 - SUPERPOSITION OF SINGLE BARS

STEP NUMBER	DEFLECTION Δ (in = 25,4 mm)	UNCRAKED STIFFNESS			CRACKED STIFFNESS		
		BAR 1	BAR 2	BAR 3	BAR 1	BAR 2	BAR 3
1	< 0.00113	X	X	X			
2	> 0.00113 < 0.00226	X	X				X
3	> 0.00226 < 0.00339	X				X	X
4	> 0.00339 < 0.01655				X	X	X
5	> 0.01655 < 0.03310				X	X	YIELDS
6	> 0.03310 < 0.04965				X	YIELDS	YIELDS
7	> 0.04965				YIELDS	YIELDS	YIELDS

X... LABELS THE STIFFNESS TO BE ADDED (SEE FIG.2.2)



a) STRUCTURE AND LOADING



ELEMENT CROSS SECTION :
 SAME AS IN FIG 1.1 (b)

LOAD : $P/2$ ACTING
 AT NODES 7 AND 8
 IN X-DIRECTION

0... ELEMENT NUMBERS
 12 CST-ELEMENTS
 8 BOUNDARY ELEMENTS
 19 NODES
 28 DOF

b) FINITE ELEMENT MESH LAYOUT

c) MATERIAL PROPERTIES : SAME AS IN EXAMPLE 1 (FIG 1.1 (c))

FIG 4.1 EXAMPLE 2 - STRUCTURE, IDEALISATION AND MATERIAL PROPERTIES
 (1" \equiv 1 in. = 25,4 mm)

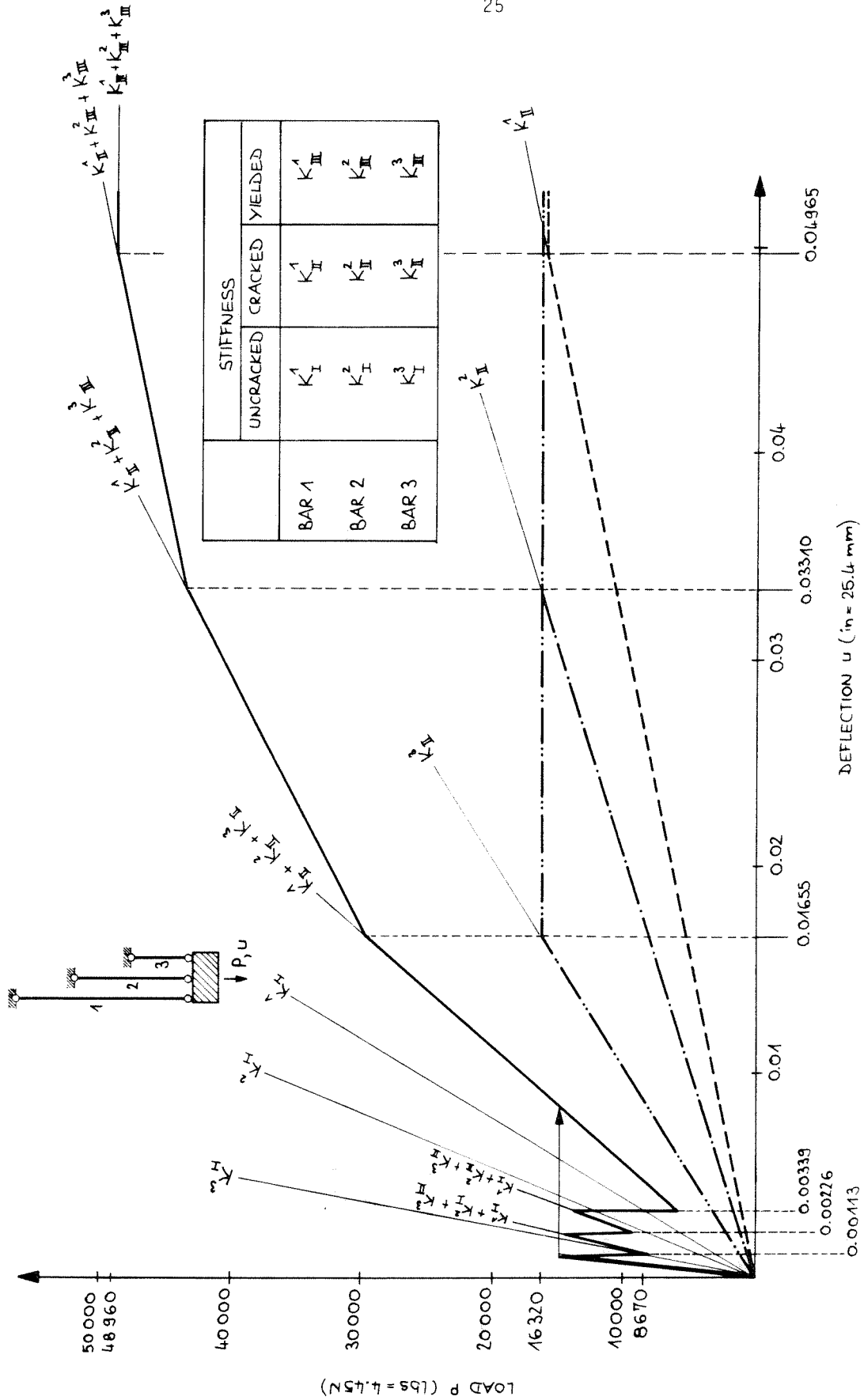


FIG 4.2 EXAMPLE 2 - CONSTRUCTION OF THE LOAD DEFLECTION CURVE BY SUPERPOSITION

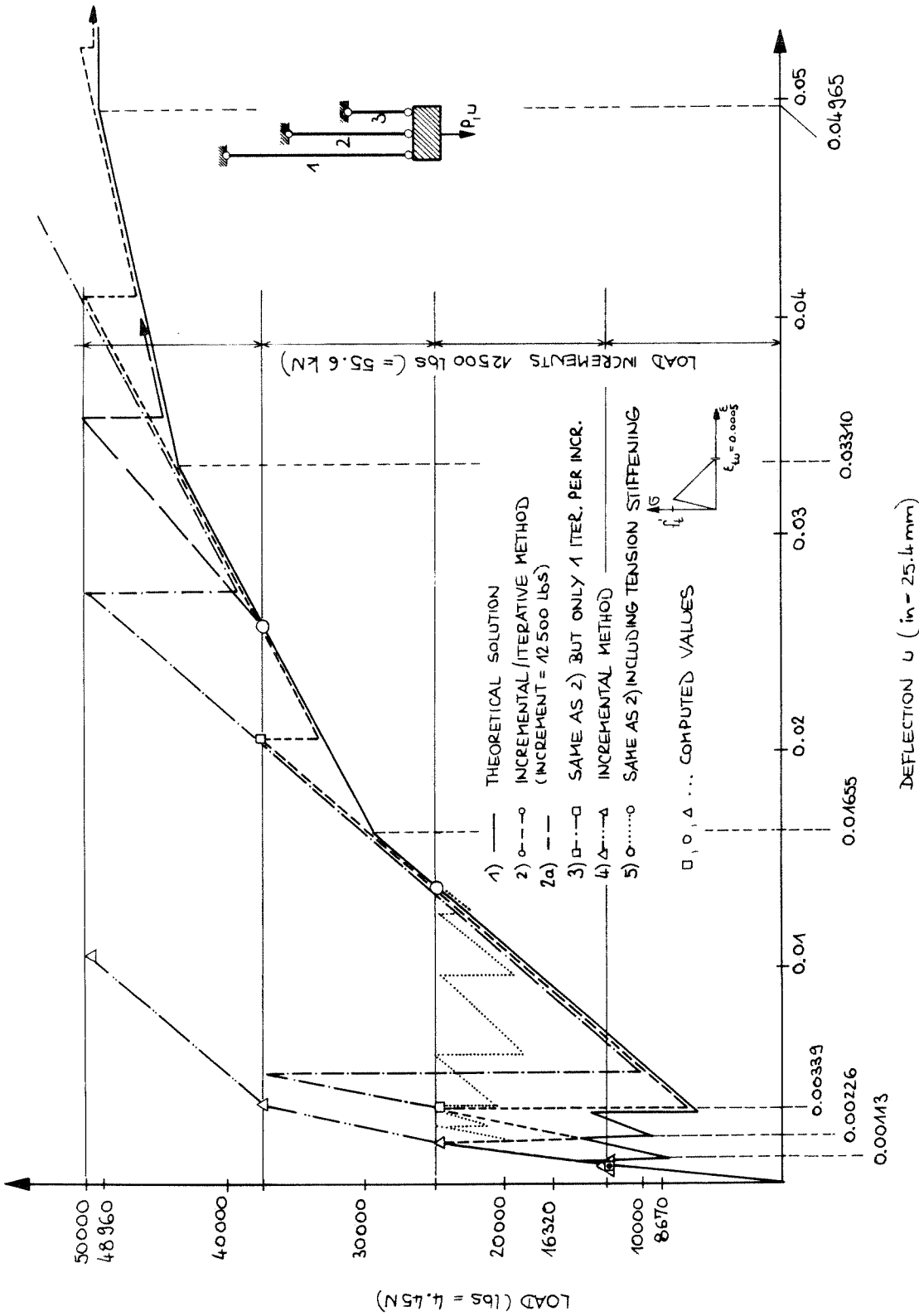
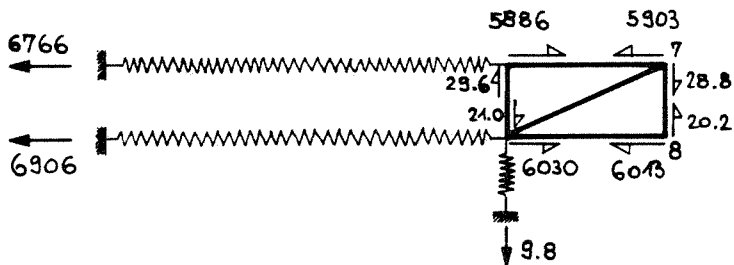
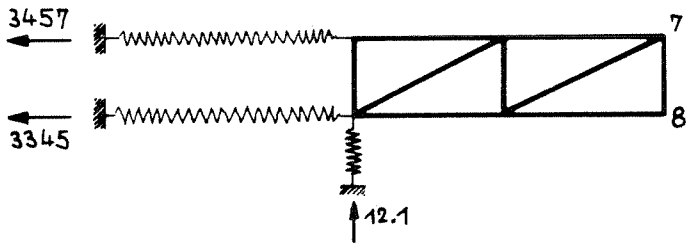
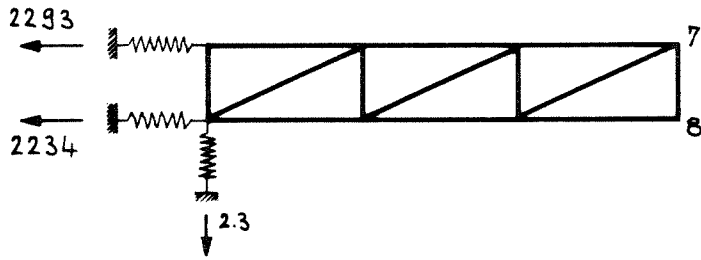


FIG. 4.3 EXAMPLE 2 - LOAD DEFLECTION CURVES



- EXTERNAL FORCES
- EXTERNAL FORCES AT NODE 7 AND 8 : 12500 lbs (= 55.6 kN)
- UNBALANCED FORCES

FIG 4.4 EXAMPLE 2 - UNBALANCED AND EXTERNAL FORCES .
SECOND INCREMENT , FIRST ITERATION

5. EXAMPLE 3 - REINFORCED CONCRETE BEAM

The beam is a more complicated system to test the program NOTACS. Since this beam is the test specimen (No. 23100) of current investigations at the Technical University of Braunschweig [11], numerical and experimental solutions are available for comparison. The research project underway in Braunschweig includes numerical and experimental studies of the behavior under sustained load. Until now (September 1977) no results for creep and shrinkage are available.

The structure and its idealization are shown in Fig. 5.1. Due to symmetry, the analysis can be performed for half of the two-span beam. To control the equilibrium of the vertical forces, boundary elements with a large extensional stiffness are chosen to simulate the supports. The upper and lower extensional reinforcement are represented by equivalent smeared steel layers. The concrete cross section is divided into eight layers of equal thickness. The stirrups are not taken into account.

The material properties given in [11] and those assumed for the analysis are presented in Fig. 5.2. The test specimens were kept at 20°C and 100% humidity during the first seven days; thereafter they were stored at the same temperature and 60% humidity.

The following input data can be determined from Fig. 5.2.

$$E_0 = 170,000 \text{ kp/cm}^2 = 1668 \text{ KN/cm}^2$$

$$f'_c = 325 \text{ kp/cm}^2 = 3.2 \text{ KN/cm}^2$$

$$\epsilon_c = 2.7\%$$

Specifications are not given for concrete in tension; therefore, the tensile strength is calculated on the basis of ACI recommendations, assuming unit weight of concrete (microconcrete) to be 110 pcf (1772 kg/m³):

$$f'_t = 17 \text{ kp/cm}^2 = 167 \text{ N/cm}^2$$

In the absence of experimental data, the rest of the properties are chosen as follows:

$$\epsilon_{ut} = 0.1 \text{ (i.e., no tension stiffening effect)}$$

$$\epsilon_{uc} = 4\%$$

$$\nu = 0.0$$

$$\beta = 1.0$$

The properties for the reinforcing steel are:

$$E_s = 20,000 \text{ kp/mm}^2 = 196,000 \text{ N/mm}^2$$

$$E_{sh} = 1/100 E_s$$

$$f_y = 59 \text{ kp/mm}^2 = 579 \text{ N/mm}^2$$

5.1 Nonlinear Analysis

First linear analyses were performed with different mesh layouts. The results varied only slightly. The load increments were chosen as:

2 at 200 kp (1.99 KN)

2 at 100 kp (0.98 KN)

12 at 200 kp (1.99 KN)

7 at 100 kp (0.98 KN)

The increments summed to a total load of 3700 kp (36.3 KN). A maximum of six iterations were allowed within one load step. The convergence was controlled by the vertical deflections. A tolerance of 10% (i.e., an error of 10% of the increment of the first iteration) led to sufficiently accurate results.

In Table 5.1 and Fig. 5.3 the load-deflection curve for the middle point is presented. The results compare sufficiently well with those

given in [11]. The deviation at the beginning of cracking is due to the assumption of a low tensile strength. Obviously, the concrete as cast had a higher actual tensile strength. At higher loads the discrepancy results from the neglected tension stiffening effect. The excellent agreement of the numerical and experimental Braunschweig solutions [11] was made possible by their adjustment of the intensity of the tension stiffening effect. The larger deviations in the vicinity of the ultimate load follow from the bilinear approximation of the steel material. The assumed stress-strain model underestimates for high stress levels the strains up to 30%. Since not all sections of the beam are under such high stresses, the effect on the load-deflection curve is less severe.

The behavior after the first cracks developed is more or less linear. This is also demonstrated in the crack patterns (Fig. 5.4). The main cracks which are responsible for the change of stiffness are already developed at a load level of $P = 600 \text{ kp}$ (5.8 KN). Only after $P = 2800 \text{ kp}$ (27.4 KN) does the deflection increase nonlinearly because the reinforcement yields. Fig. 5.5 displays some deflection and bending moment profiles. It can be noted that the deflections are quite different, but the moments show little redistribution.

TABLE 5.1 - EXAMPLE 1 - LOAD DEFLECTION RELATION

INCREMENT ($k_p = 9.81N$)	TOTAL LOAD ($k_p = 9.81N$)	NUMBER OF ITERATIONS	DEFLECTION δ OF NODES 17,18 (mm)	INCREMENT OF DEFLECTION (mm)
200*	200	2	0.089	0.085
200	400	6 (a)	0.303	0.214
100	500	3	0.390	0.087
100	600	4	0.496	0.106
200	800	3	0.685	0.189
200	1000	2	0.865	0.180
200	1200	2	1.046	0.179
200	1400	2	1.227	0.181
200	1600	2	1.408	0.181
200	1800	2	1.587	0.179
200	2000	2	1.767	0.180
200	2200	2	1.945	0.178
200	2400	2	2.125	0.180
200	2600	2	2.305	0.180
200	2800	2 (b)	2.486	0.191
200	3000	3	2.852	0.356
100	3100	4	3.686	0.834
100	3200	4	4.679	0.993
100	3300	4 (c)	6.558	1.879
100	3400	3 } (d)	9.017	2.459
100	3500	2 }	11.704	2.687
100	3600	4	15.382	3.678
100	3700	2	COMPUTATION STOPPED	

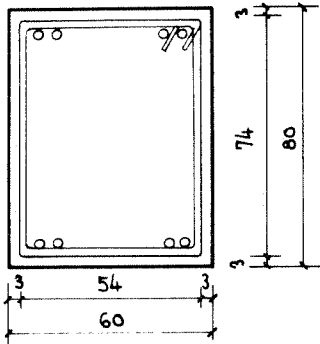
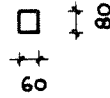
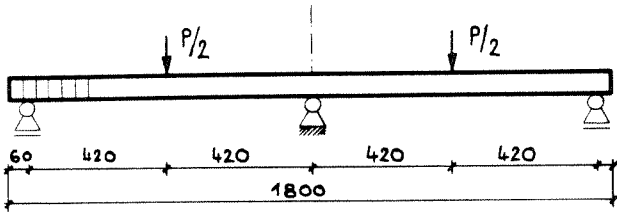
(a) FIRST CRACKS MIDSPAN AND AT FIXED SUPPORT

(b) TOP REINFORCEMENT AT FIXED SUPPORT YIELDS

(c) BOTTOM REINFORCEMENT AT MIDSPAN YIELDS

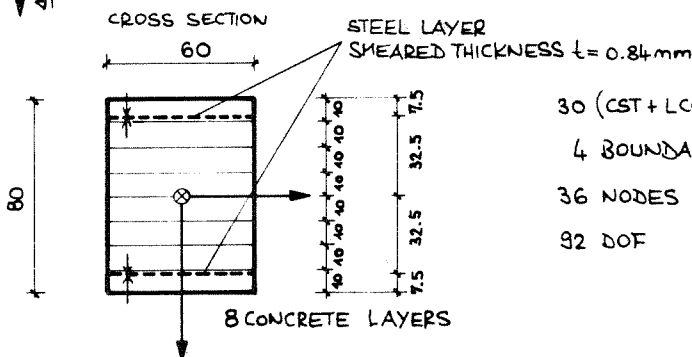
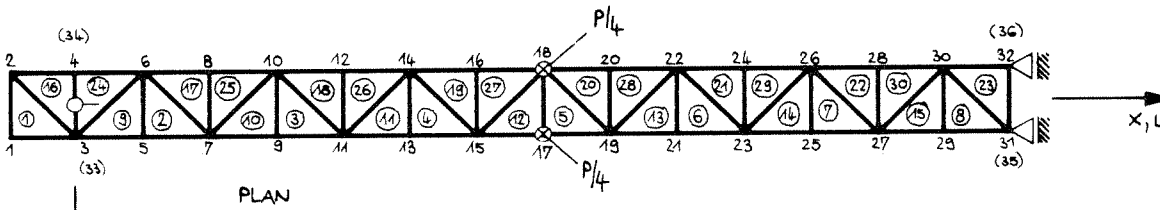
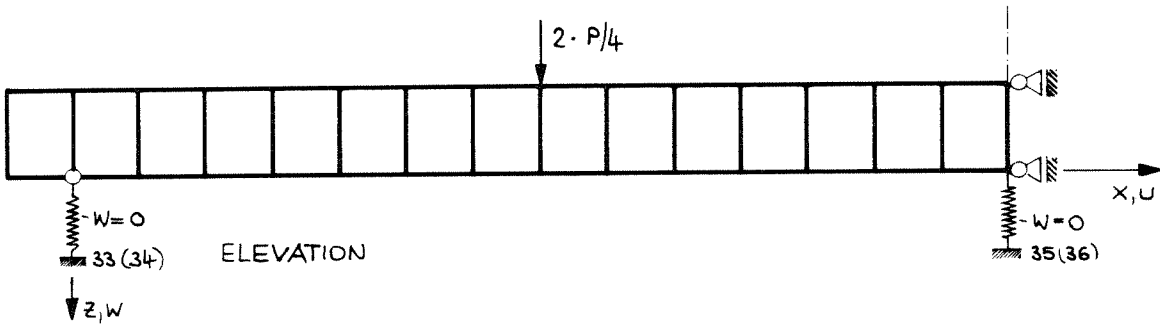
(d) OUTER CONCRETE LAYER AT MIDSPAN AND AT FIXED SUPPORT EXCEEDS COMPRESSIVE STRENGTH

* DEAD LOAD INCLUDED IN FIRST INCREMENT (VERY LOW)



LONGITUDINAL REINFORCEMENT
 8 \varnothing 4mm, BST 50/55 RK
 STIRRUPS:
 \varnothing 3mm, e = 30mm, BST 50/55 GK
 REINFORCEMENT RATIO $\rho = 2\%$
 50 ... YIELD STRENGTH
 55 ... ULTIMATE STRENGTH
 R ... DEFORMED BAR
 G ... PLAIN BAR
 K ... COLD FORMED

a) STRUCTURE AND LOADING

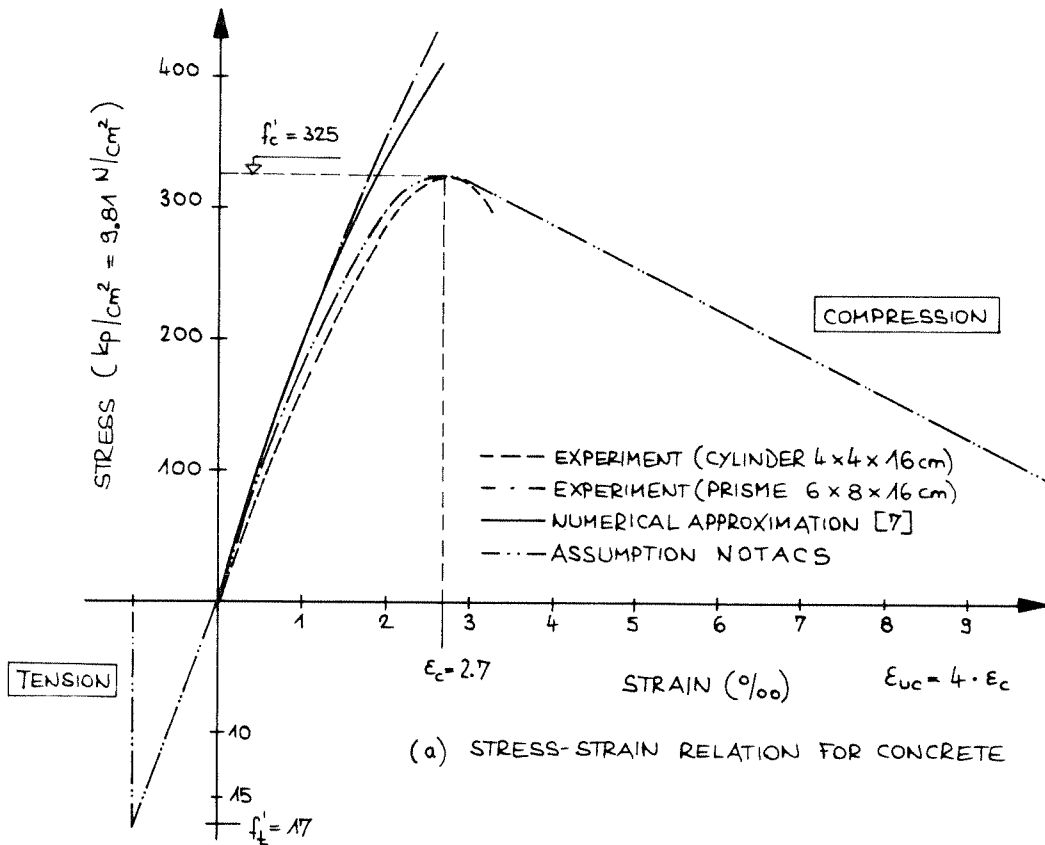


30 (CST + LCCTg) - ELEMENTS
 4 BOUNDARY ELEMENTS
 36 NODES
 92 DOF

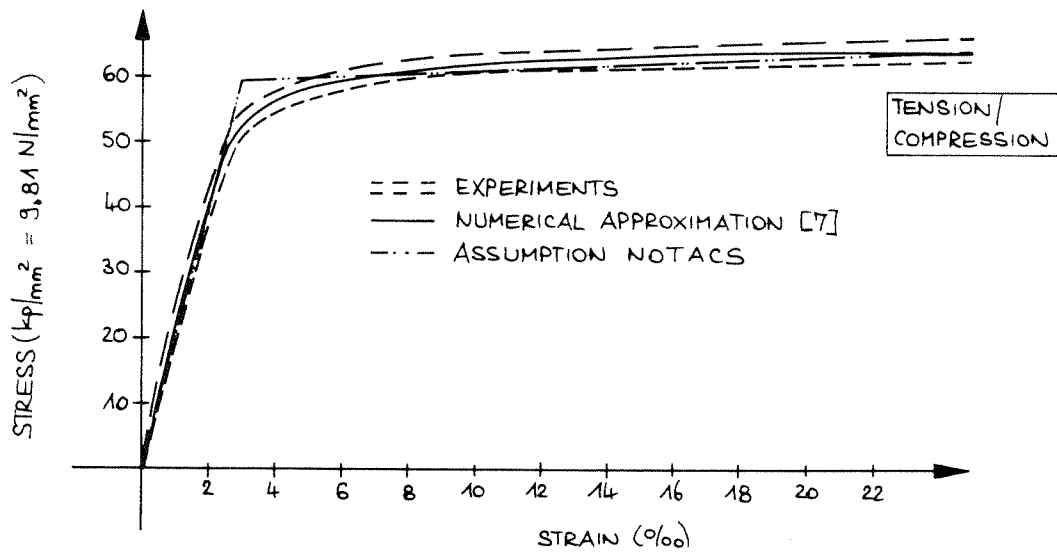
b) FINITE ELEMENT MESH LAYOUT (LEFT HALF)

ALL DIMENSIONS IN mm !

FIG 5.1 EXAMPLE 3 - STRUCTURE AND IDEALIZATION



(a) STRESS-STRAIN RELATION FOR CONCRETE



(b) STRESS-STRAIN RELATION FOR STEEL

FIG 5.2 EXAMPLE 3 - MATERIAL PROPERTIES

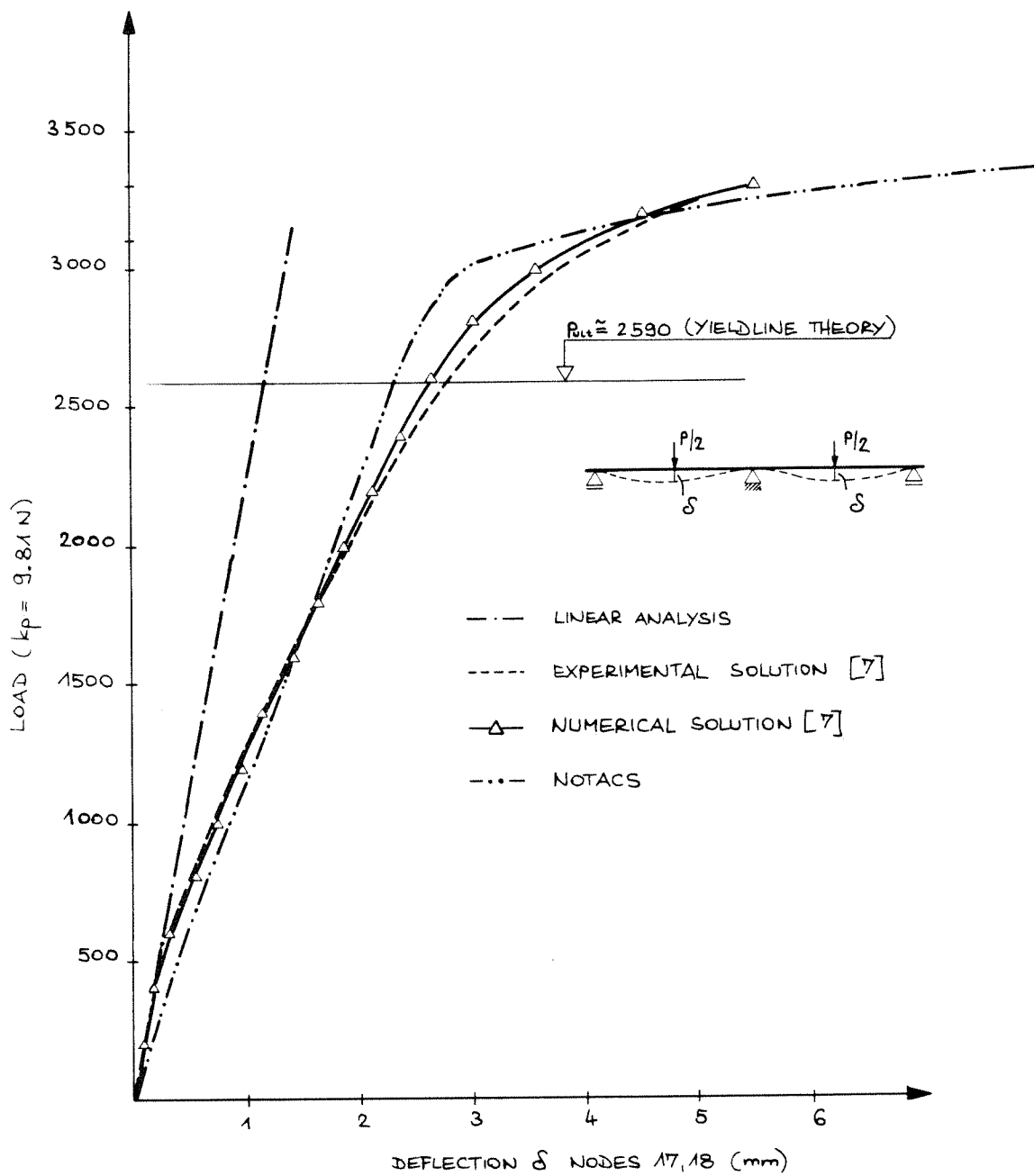


FIG 5.3 EXAMPLE 3 - LOAD DEFLECTION CURVES

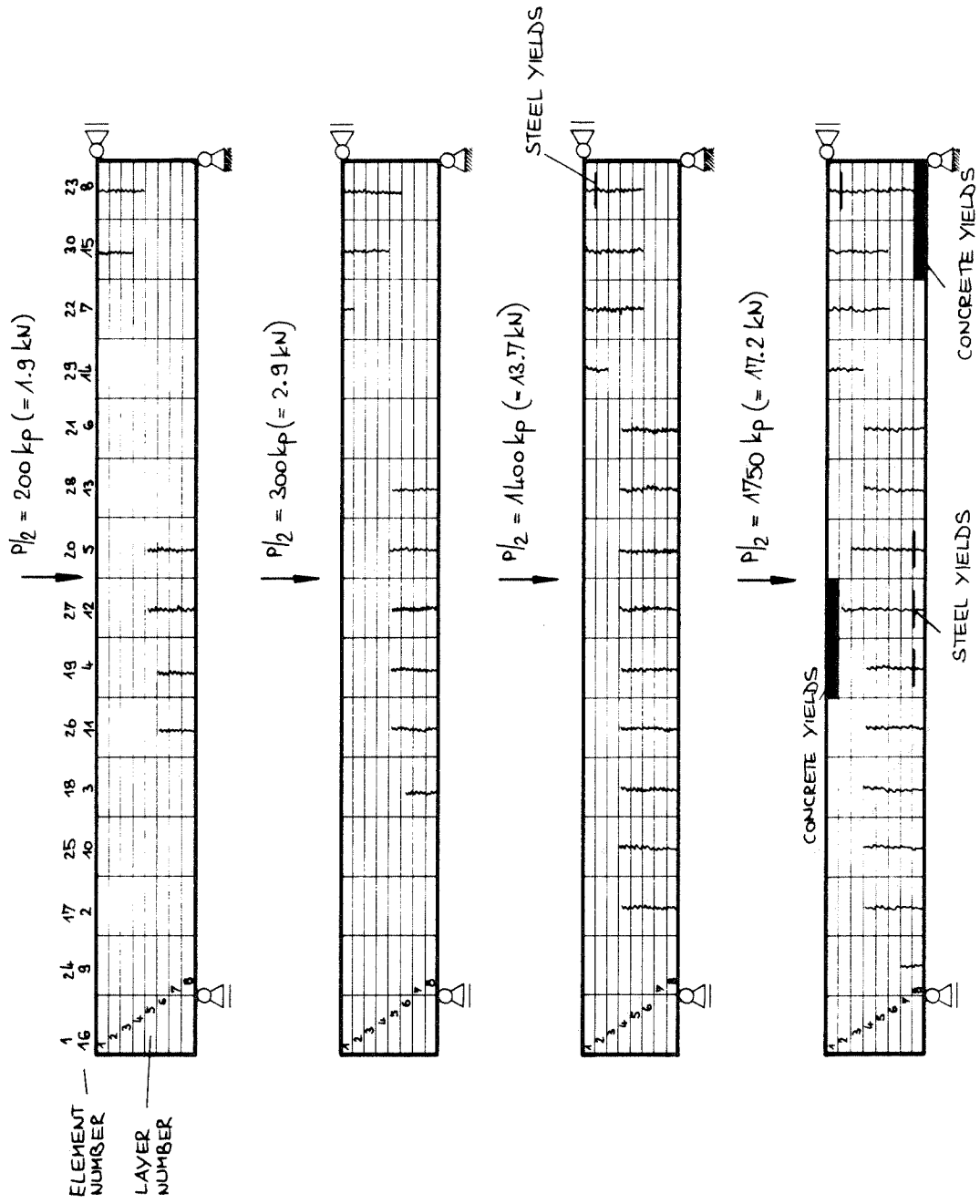


FIG 5.4 EXAMPLE 3 - CRACK PROPAGATION

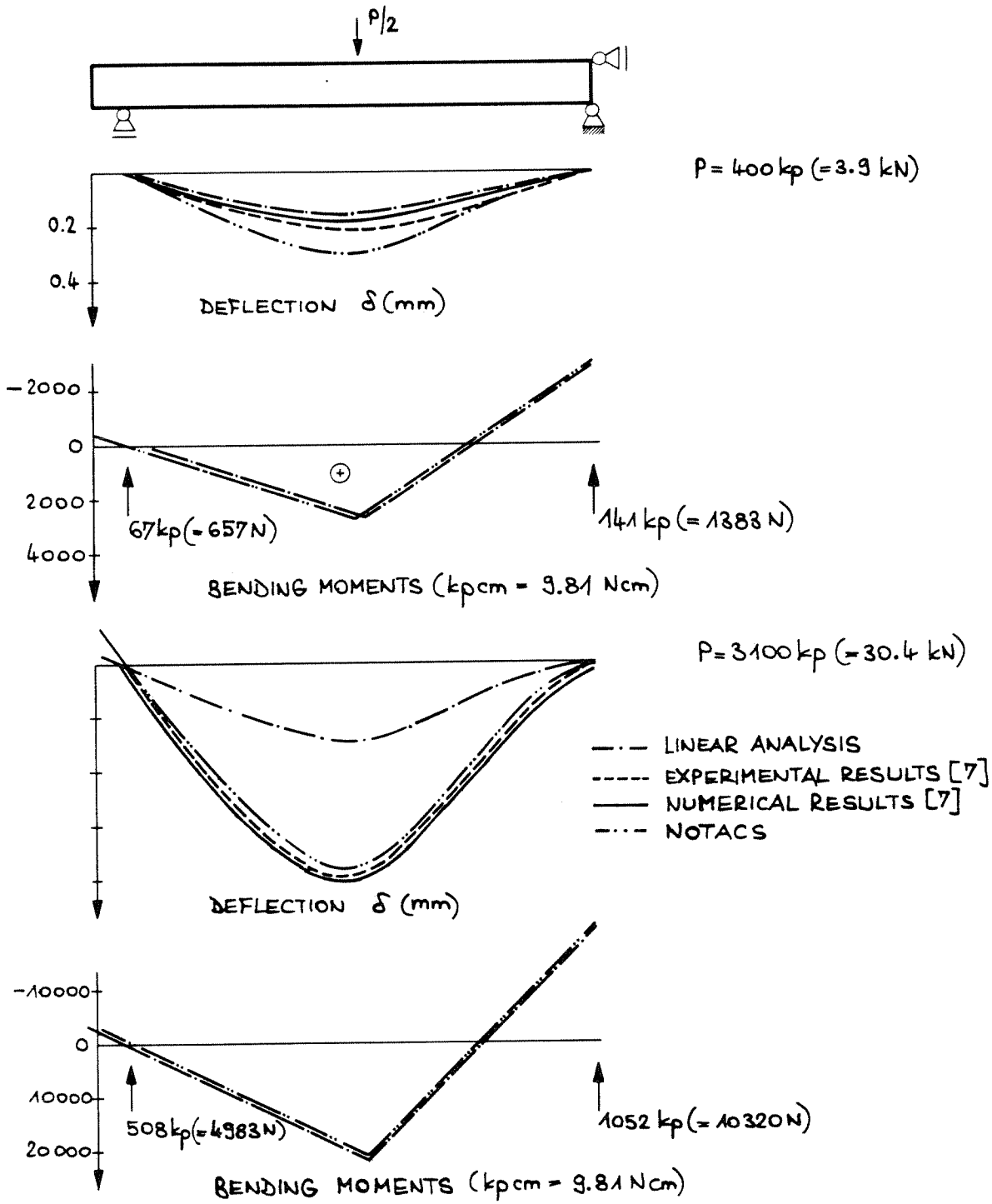
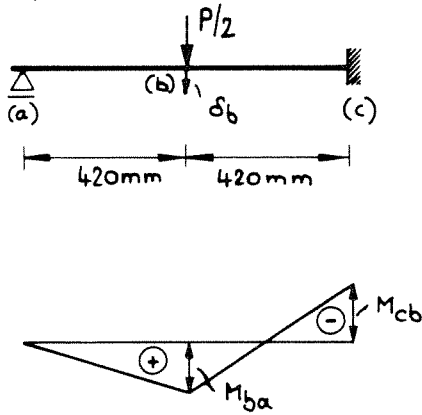
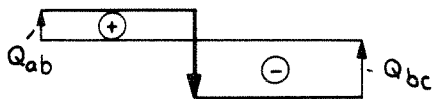


FIG 5.5 EXAMPLE 3 - DEFLECTIONS AND BENDING MOMENTS

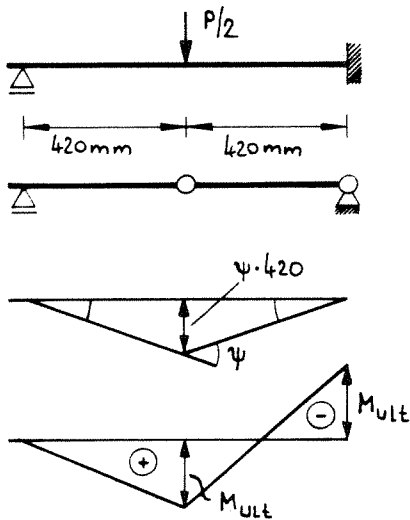
a) LINEAR ANALYSIS



LOAD	Q _{ab}	Q _{bc}	M _{ba}	M _{cb}	δ _b
k _p = 9.81 N			k _p cm = 9.81 Ncm		mm
400	64	-136	2624	-3152	0.17
3100	496	-1054	20336	-24428	1.33
3500	560	-1190	22960	-27580	1.51



b) PLASTIC ANALYSIS



SYSTEM

COLLAPSE MECHANISM

VIRTUAL DISPLACEMENT

$$\begin{aligned}
 \text{VIRTUAL EXTERNAL WORK : } \delta A_e &= P/2 \cdot \psi \cdot 420 \\
 \text{VIRTUAL INTERNAL WORK : } \delta A_i &= (M_{ult} \cdot 2 + M_{ult}) \bar{\psi} \\
 &> \delta A_e + \delta A_i = 0 \\
 &\Rightarrow P_{ult} = 0.0143 M_{ult}
 \end{aligned}$$

ACI FORMULA PREDICTS AN ULTIMATE BENDING MOMENT OF

$$M_{ult} = 18\,092 \text{ kpcm} (= 172\,000 \text{ Ncm}) \text{ HENCE } P_{ult} \approx 2590 \text{ kp} (= 25.4 \text{ kN})$$

FIG 5.6 EXAMPLE 3 HAND-CALCULATION (CONTROL)

6. EXAMPLE 4 - REINFORCED CONCRETE SLAB

This system is used to test the program on a two-dimensional problem. The structure is also being studied in the investigations underway in Braunschweig [11], where it is intended to study the behavior under instantaneous and sustained load conditions, numerically as well as experimentally. The plate (Fig. 6.1) is simply supported at the four corners and is loaded by a concentrated force in the center. The top and bottom reinforcement extend throughout the plate in both directions. The information on material properties in [11] is rather scarce. Reasonable assumptions and code specifications have been used to determine the material data not given (Fig. 6.2).

Lightweight Concrete:

$$E_o = 16,400 \text{ N/mm}^2 \text{ (2380 ksi)}$$

$$f'_c = 43 \text{ N/mm}^2 \text{ (6.23 ksi)}$$

$$\epsilon_c = 2.7\%$$

$$f'_t = 2 \text{ N/mm}^2 \text{ (290 psi)}$$

$$\epsilon_{ut} = 0.12\%$$

$$\epsilon_{uc} = 4 \epsilon_c$$

$$\nu = 0.0$$

$$\beta = 0.5$$

Steel:

$$E_s = 201,000 \text{ N/mm}^2 \text{ (29,000 ksi)}$$

$$E_{sh} = 0$$

$$f_y = 670 \text{ N/mm}^2 \text{ (97 ksi)}$$

The finite element idealization is presented in Fig. 6.3. Due to symmetry, the analysis can be performed on an eighth of the structure.

Along the symmetry edges, appropriate boundary elements with large rotational or extensional stiffnesses are used.

6.1 Nonlinear Analysis

The procedure and the choice of the tolerances are the same as for Example 3. The load is divided into 23 increments (Fig. 6.4 and Table 6.1). At $P = 12$ KN the maximum number of iterations (6) was needed since intensive cracking started at that load level. However, it was observed that the residual unbalanced forces were very small compared to the total nodal forces, i.e., the solution obtained is sufficiently accurate from an equilibrium standpoint. For the same reasons as discussed in Example 3, the load-deflection curve does not match exactly the results obtained in Braunschweig [11]. First of all, the true tensile strength is obviously much higher than the assumed one. Also, the tensile stiffening effect is more significant. One reason for this is the lower reinforcement ratio. Again, the discrepancy at higher loads is due to the coarse approximation of the steel stress-strain relation. However, even though the true approximated strains differ by more than 100% at stresses of about 670 N/mm^2 , the differences in the load deflection curves are not more than 15%. The ultimate load is reached at about 62 KN for both solutions. Yielding of steel starts in the middle of the plate at a load of about 48 KN and propagates thereafter on the center lines to the edges. The concrete first reaches its compressive strength at the centers of the edges. This seems reasonable since the concrete in these areas is stressed mainly uniaxially and thus shows a lower compressive strength as compared to the middle areas of the plate where it is stressed biaxially.

Crack patterns are shown in Fig. 6.5, where it can be seen that they form almost exclusively on the bottom of the plate. Around the concentrated external force at the center of the plate, radial as well as tangential cracking occurs even at a relatively low load level. Near the corner support reactions, the cracks build up much later. In Fig. 6.6 deflection and moment profiles for $P = 40$ KN are depicted. In [11] values are only given for the deflections along line ME, Fig. 6.6. These values are in excellent agreement with those obtained by NOTACS.

6.2 Hand Calculation (Control)

The control is demonstrated in Fig. 6.7. Referring to the linear analysis, the action loads compare sufficiently well with the reaction forces. A limit analysis based on yield line theory predicts an ultimate load of $P_{ult} = 53$ KN, which is less than the actual.

TABLE 6.1 EXAMPLE 4 - LOAD DEFLECTION RELATION

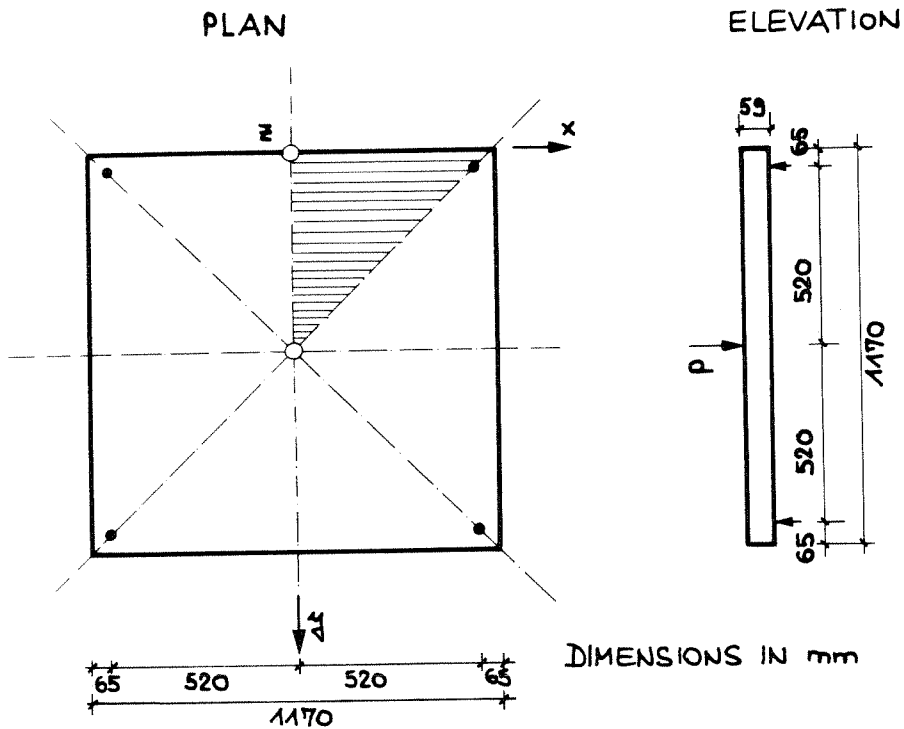
INCREMENT (kN)	TOTAL LOAD (kN)	NUMBER OF ITERATIONS	DEFLECTION OF NODE 28 (mm)	INCREMENT OF DEFLECTION (mm)
4	4 *	2	0.455	0.455
4	8	2	0.859	0.404
4	12	6(a)	2.869	2.010
2	14	4	3.447	0.578
2	16	3	4.027	0.580
2	18	3	4.763	0.736
2	20	2	5.337	0.574
4	24	2	6.423	1.086
4	28	2	7.519	1.096
4	32	2	8.619	1.100
4	36	2	9.726	1.107
4	40	2	10.820	1.094
4	44	2	11.913	1.093
2	46	2	12.456	0.543
2	48	2(b)	13.008	0.552
2	50	2	13.584	0.576
2	52	2	14.219	0.634
2	54	2	14.866	0.648
2	56	3	15.652	0.786
2	58	3	16.490	0.838
2	60	2	17.285	0.795
2	62	4(c)	18.174	0.889
2	64	5	23.062	4.888

(a) FIRST CRACKS

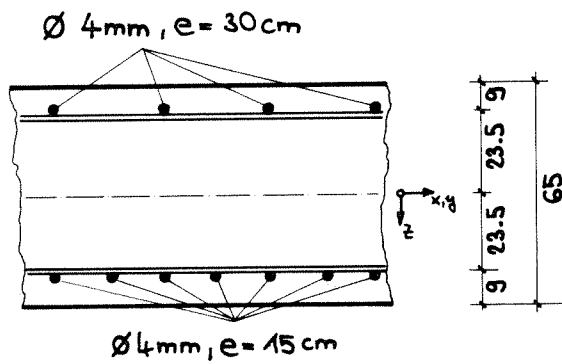
(b) BOTTOM REINFORCEMENT IN ELEMENT 36 YIELDS

(c) CONCRETE EXCEEDS COMPRESSION STRENGTH (ELEMENTS 7, 13),
SPREADING OF YIELDING

* DEAD LOAD INCLUDED IN FIRST INCREMENT (VERY LOW)



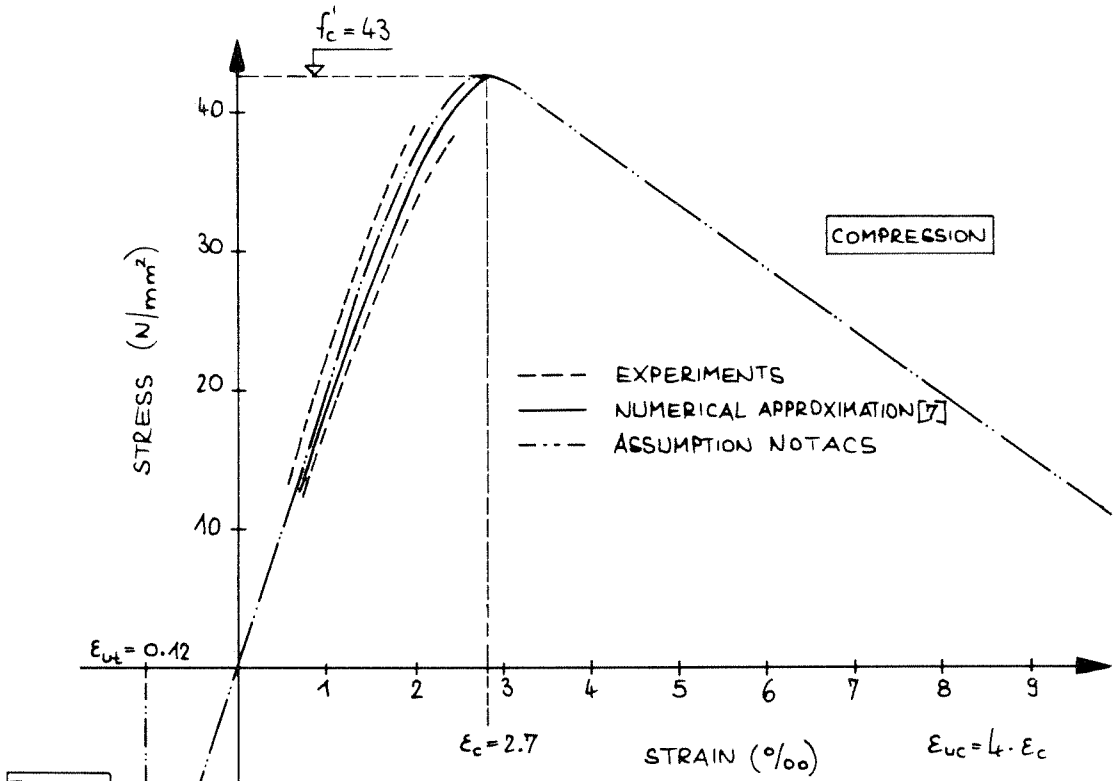
CROSS SECTION (SAME IN x- AND y- DIRECTION)



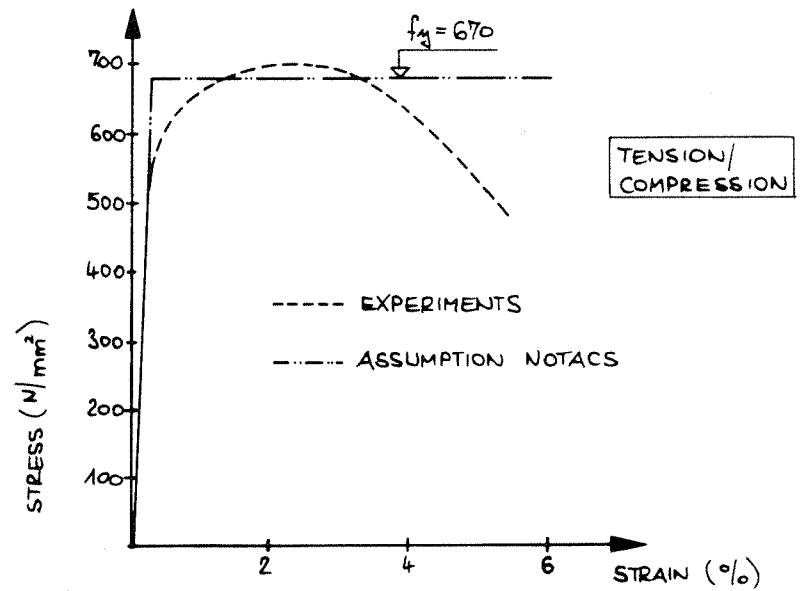
UPPER REINFORCEMENT : BST 50/55 RK ; $A_s = 1.93 \text{ cm}^2/\text{m}$; $\rho = 0.3\%$
 LOWER REINFORCEMENT : BST 50/55 RK ; $A_s = 3.97 \text{ cm}^2/\text{m}$; $\rho = 0.6\%$

50 ... YIELD STRENGTH
 55 ... ULTIMATE STRENGTH
 R ... DEFORMED BAR
 K ... COLD-FORMED

FIG 6.1 EXAMPLE 4 - STRUCTURE AND LOADING



a) STRESS-STRAIN RELATION FOR CONCRETE



b) STRESS-STRAIN RELATION FOR STEEL

FIG 6.2 EXAMPLE 4 MATERIAL PROPERTIES

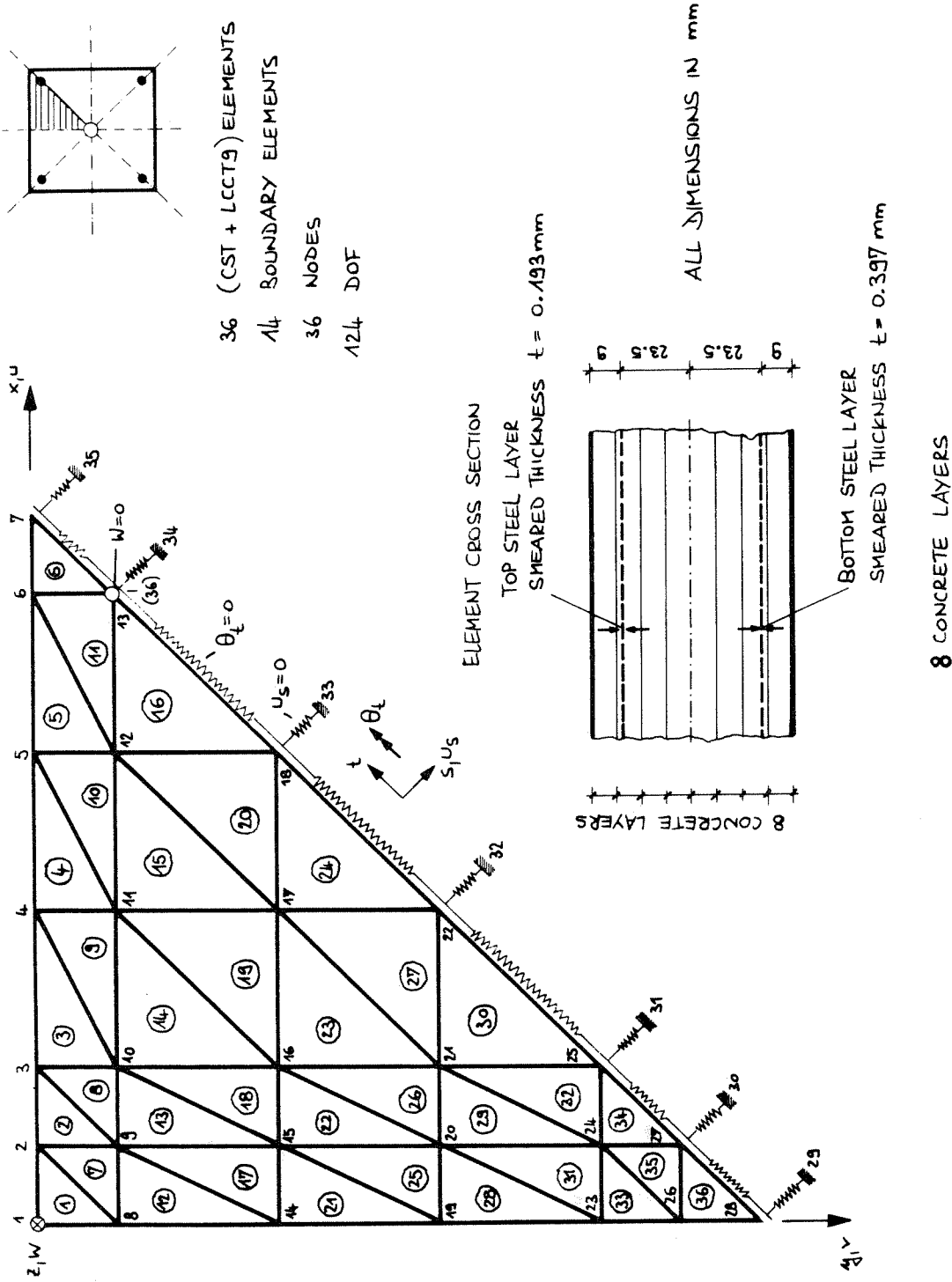


FIG 6.3 EXAMPLE 4 - FINITE ELEMENT MESH LAYOUT

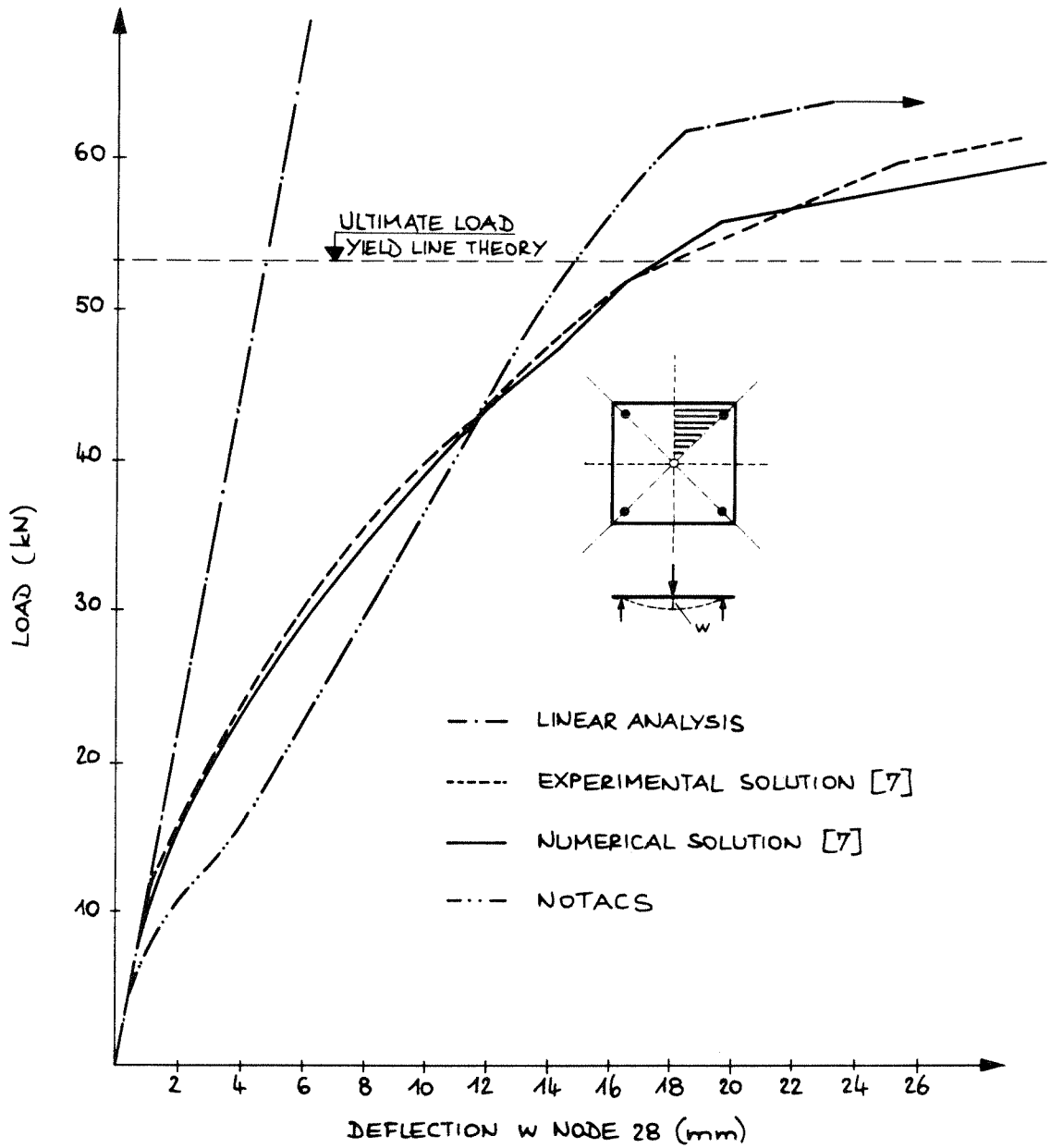
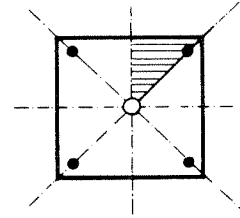
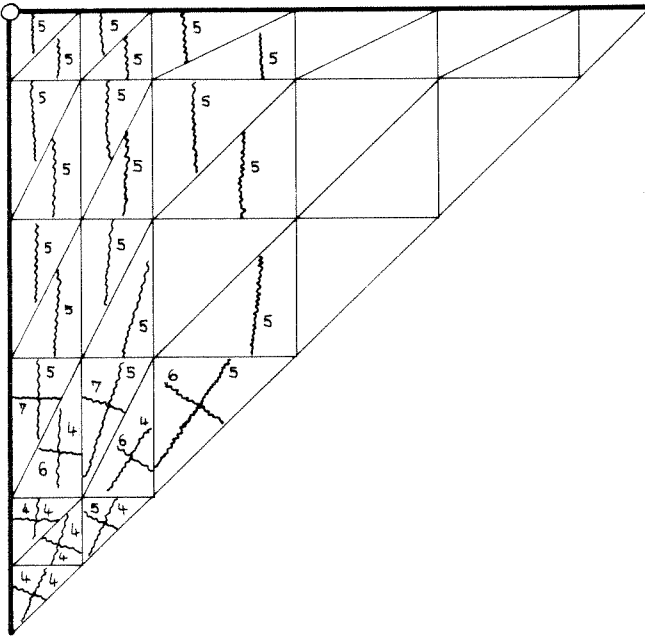
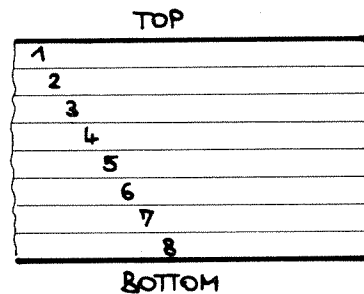
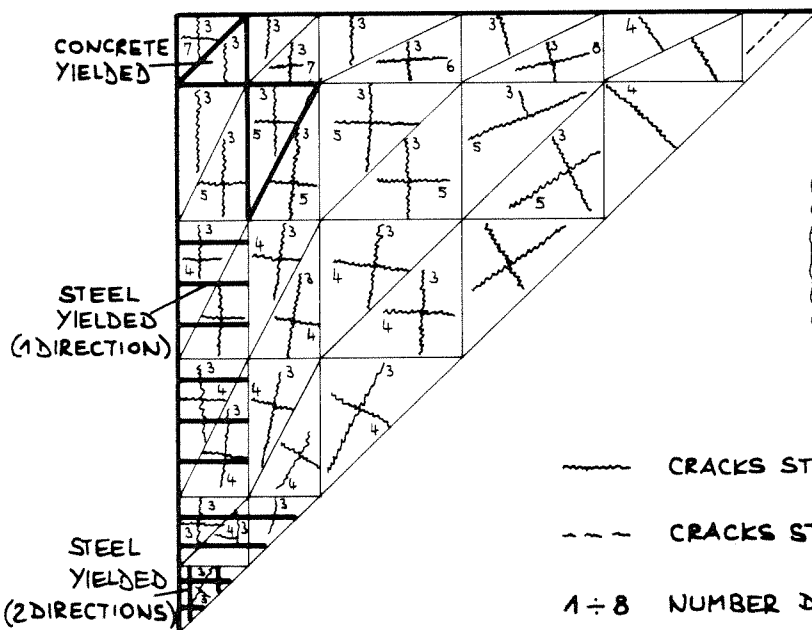


FIG 6.4 EXAMPLE 4 - LOAD DEFLECTION CURVES

$P = 12 \text{ kN}$



$P \approx 62 \text{ kN}$



- CRACKS START AT THE BOTTOM LAYER
- - - CRACKS START AT THE TOP LAYER
- 1 ÷ 8 NUMBER DEFINE CRACK DEPTH

FIG 6.5 EXAMPLE 5 - CRACK PROPAGATION

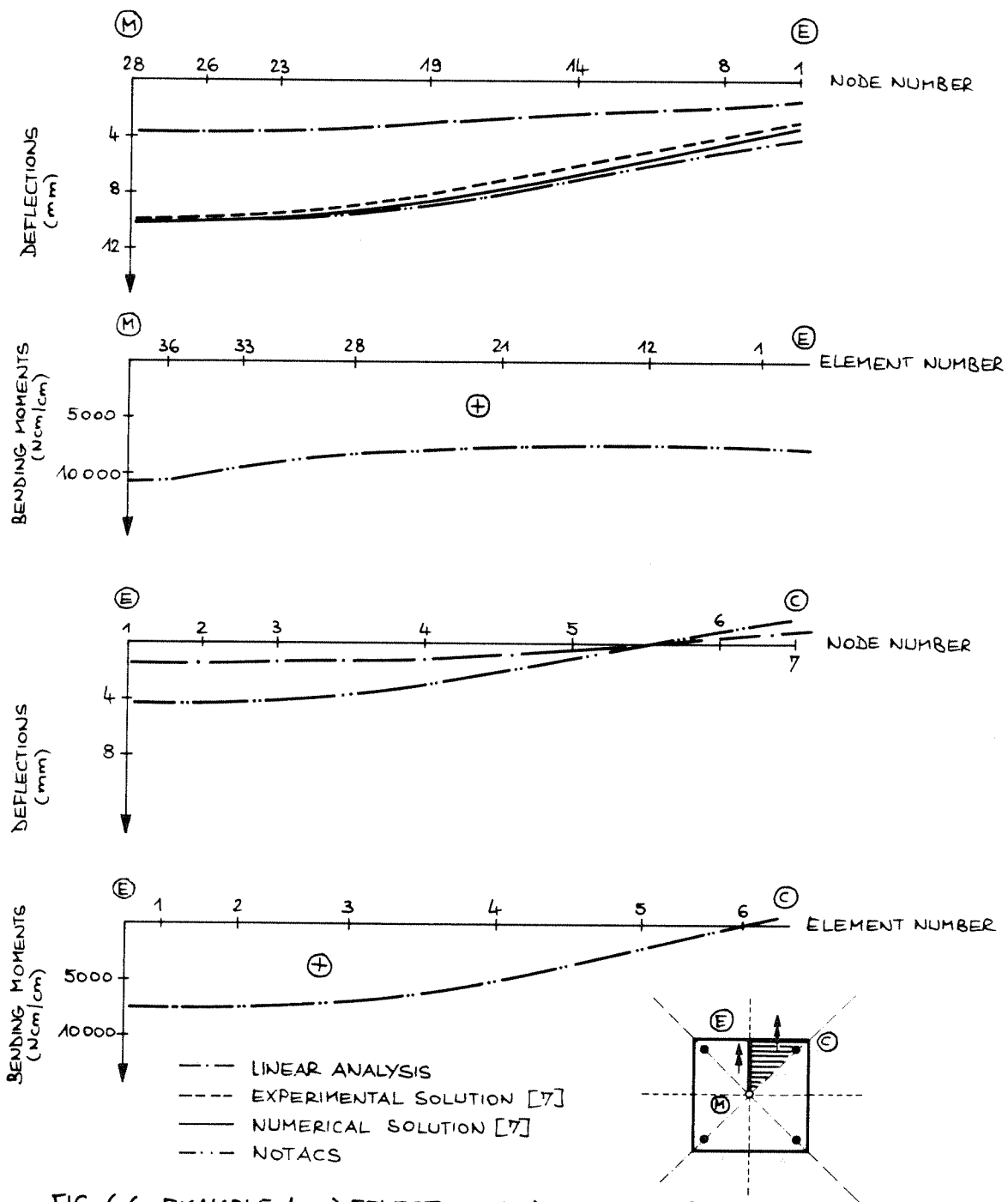
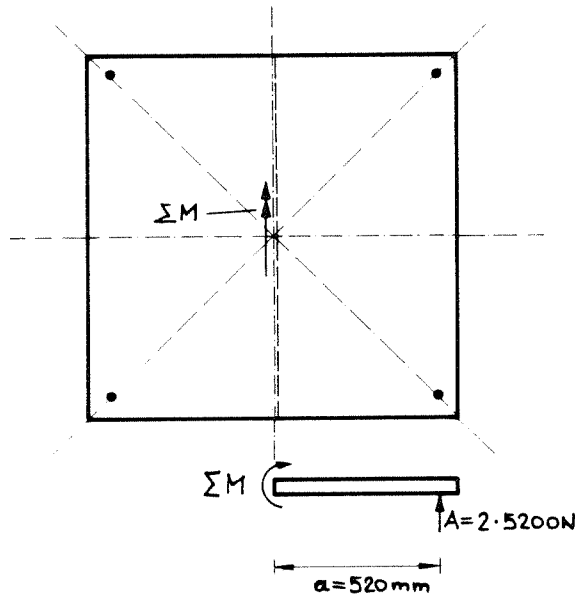


FIG 6.6 EXAMPLE 4 - DEFLECTION AND MOMENT PROFILES

(a) LINEAR ANALYSIS (e.g. $P = 40 \text{ kN}$)



Σ VERTICAL FORCES = 0 ?

ACTION \equiv LOAD

DEAD LOAD : 190 N

LIVE LOAD : 40000 N

TOTAL LOAD : 40190 N

REACTION \equiv SUPPORT FORCES

$4 \cdot 2 \cdot 5200 \text{ N} = 41600 \text{ N}$

\approx EQUILIBRIUM !

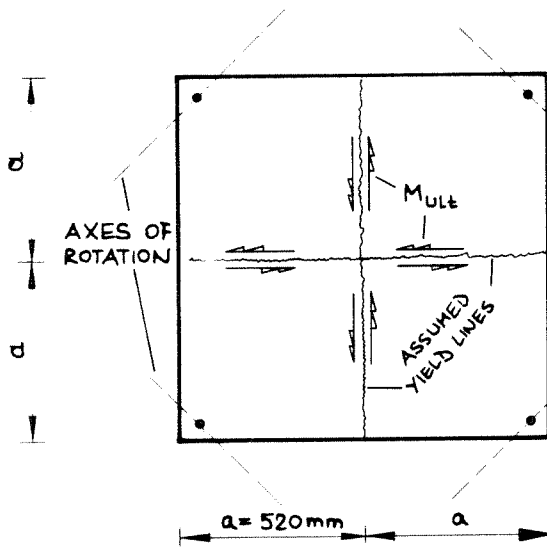
Σ MOMENTS ALONG CENTER LINE = 0 ?

$\Sigma M \approx 10.4 \text{ kNm}$

$2 \cdot A \cdot a = 2 \cdot 10400 \cdot 520 = 10.8 \text{ kNm}$

\approx EQUILIBRIUM !

(b) YIELD LINE THEORY



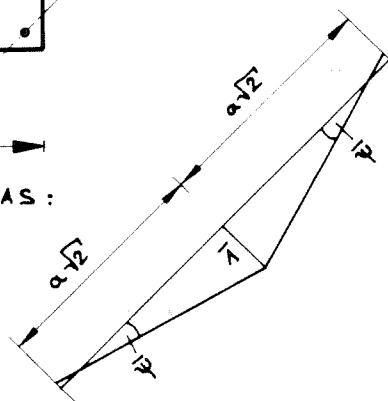
VIRTUAL INTERNAL WORK :

$$\delta A_i = 4 (M_{ult} \cdot \sqrt{2} \cdot a \cdot \bar{\psi})$$

VIRTUAL EXTERNAL WORK :

$$\delta A_e = P \cdot \bar{1}$$

$$\delta A_i = \delta A_e \rightarrow \underline{\underline{P_{ult} = 4 M_{ult}}}$$



M_{ult} ACCORDING TO ACI FORMULAS :

$$M_{ult} = 13.1 \text{ kNm/m}$$

$$\underline{\underline{P_{ult} \approx 53 \text{ kN}}}$$

FIG 6.7 EXAMPLE 4 HAND-CALCULATION (CONTROL)

7. RECOMMENDATIONS FOR EXTENSION OF THE PROGRAM AND FOR FURTHER STUDIES

In the following comments some suggestions for possible improvement and extension of the computer program NOTACS are listed in an arbitrary sequence.

- (1) Implementation of a more powerful equation solver.--The nonlinear analysis requires the solution of a great number of sets of equations; therefore, a fast equation solver is extremely important. The subroutine SYMSOL which is used in the program could be replaced by one of the more sophisticated subroutines such as OPTSOL developed by Professor G. H. Powell [12] or SESOL developed by Professor E. L. Wilson [13]. Newer versions of both subroutines, namely CHOSOP and SORE, respectively, are currently being developed.
- (2) Modification of the finite element.--The shell element in NOTACS is a combination of a CST and a LCCT9 element. It is widely recognized that the CST element is too simple to represent the membrane state of stress whereas the LCCT9 element yields good results.
- (3) Implementation of a restart option.--The correct choice of the number of load steps, time steps, and required iterations and the optimal choice of the tolerances is not an easy task, even with some previous experience with the program. Each new problem may require a different combination to get the best solution. A restart option is thus advantageous because it is then possible to stop the analysis at an intermediate state without losing the results already obtained.
- (4) Revision of the program.--The program should be revised again. As suggestions, the input should be a bit more systematically organized, the echo print should be completed, it should be possible to work with

arbitrary dimensions, and the programming language should be standard (FORTRAN IV).

(5) Incorporation of geometric nonlinearity.--Geometric nonlinearity can be an important factor in determining the true nonlinear response of various shell type structures. As a first step, the external geometric stiffness (P- Δ effect) could be included.

(6) Modification of stress-strain relation of steel.--The assumed bilinear stress-strain relation should be exchanged by a trilinear or multilinear relation.

(7) Modification of stress-strain relation of concrete.--It is questionable if the biaxial behavior is really worth the effort needed. The major contributor to the nonlinear behavior of reinforced concrete structures is the tensile cracking. To answer this question, solutions obtained by a simple uniaxial elastic-plastic stress-strain relation should be compared to solutions using the original biaxial stress-strain relation.

(8) Behavior of reinforced concrete in tension.--Extensive experimental and numerical studies are necessary to develop a more realistic constitutive model of reinforced concrete in tension. More information is needed to determine the tensile strength, the tension stiffening curve, and the cracked shear modulus. References [5], [6], [7], [9], [10], and [14] might be helpful to this end.

(9) Long time behavior.--The numerical analysis of time dependent and environmental effects is at the very beginning. For creep and shrinkage more sophisticated models have to be investigated.

(10) Prestressing.--Prestressing may be incorporated in this program as shown in [15] for one-dimensional beam and frame problems.

(11) Application of the present program on structural systems.--Further studies may be carried out for various problems to study the behavior under both instantaneous and sustained loads, e.g., flat slabs, skew slabs, and slabs with discontinuous supports.

8. REFERENCES

- [1] Kabir, A. F., "Nonlinear Analysis of Reinforced Concrete Panels, Slabs and Shells for Time-Dependent Effects," UC-SESM Report No. 76-6, University of California, Berkeley, December 1976.
- [2] Scordelis, A. C., "Finite Element Analysis of Reinforced Concrete Structures," Proceedings of the Specialty Conference on the Finite Element Method in Civil Engineering, Montreal, June 1-2, 1972, pp. 71-113.
- [3] Müller, G., "Nonlinear Analysis of Reinforced Concrete Hyperbolic Paraboloid Shells," UC-SESM Report No. 77-6, University of California, October 1977.
- [4] Schnobrich, W. C., "Behavior of Reinforced Concrete Predicted by Finite Element Method," Proceedings of the Second National Symposium on Computerized Structural Analysis and Design, George Washington University, Washington, D.C., March 1976.
- [5] Wegner, R., "Finite Element Models for Reinforced Concrete," Proceedings of the U.S.-Germany Symposium on Formulations and Computational Methods in Finite Element Analysis, Massachusetts Institute of Technology, Cambridge, August 1976.
- [6] Eibl, I. and Ivanyi, G., "Studie zum Trag- und Verformungsverhalten von Stahlbeton," Deutscher Ausschuss für Stahlbeton, Heft 260, W. Ernst & Sohn, Berlin, 1976.
- [7] Geistefeldt, H., "Constitutive Equations for Cracked Reinforced Concrete Based on a Refined Model," Paper H 4/b, Proc. 4th SMIRT-Conference, San Francisco, August 15-19, 1977.
- [8] Rostásy, F. S. and Alda, W., "Rissbreitenbeschränkung bei zentrischem Zwang von Stäben aus Stahlbeton und Stahleleichtbeton," Beton und Stahlbetonbau, 72, Heft 6, 1977, pp. 149-156.
- [9] Wegner, R., "Tragverhalten von Stahlbetonplatten mit nichtlinearen Materialgesetzen im gerissenen Zustand - Finite Element Methode," Bericht Nr. 74-11, Institut für Statik, TU Braunschweig, 1974.
- [10] Koch, R., "Verformungsverhalten von Stahlbetonstäben unter Biegung und Längszug im Zustand II auch bei Mitwirkung des Betons zwischen den Rissen," Schriftenreihe Otto-Graf-Institut, Heft 69, 1976.
- [11] Duddeck, H., Griebenow, G., and Schaper, G., "Auszüge aus dem sechsten Arbeitsbericht zum Forschungsvorhaben Stahlbetonplatten mit nichtlinearen Stoffgesetzen," Arbeitsbericht Institut für Statik, TU Braunschweig, 1976.
- [12] Powell, G. H. and Mondkar, D. P., "Large Capacity Equation Solver for Structural Analysis," Computers and Structures, 4, 1974, pp. 699-778.

- [13] Wilson, E. L., Bathe, K. J., and Doherty, W. P., "Direct Solution of Large Systems of Linear Equations," Computers and Structures, 4, 1974, pp. 363-372.
- [14] Arbeitsgruppe Massivbau Darmstadt, "Forschungsberichte," Nr. 15, 16, 25, Institut für Massivbau, TH Darmstadt, 1974.
- [15] Kang, Y. J., "Nonlinear Geometric, Material and Time Dependent Analysis of Reinforced and Prestressed Concrete Frames," UC-SESM Report No. 77-1, University of California, Berkeley, January 1977.